

Group B streptococcal membrane vesicles induce proinflammatory cytokine production and are sensed in an NLRP3 inflammasome-dependent mechanism in human macrophages

Cole R. McCutcheon <sup>1</sup>, Jennifer A. Gaddy <sup>2,3,4</sup>, David M. Aronoff <sup>5</sup>,  
Shannon D. Manning <sup>1\*</sup>, and Margaret G. Petroff <sup>1,6\*</sup>

<sup>1</sup> Department of Microbiology and Molecular Genetics, Michigan State University, East Lansing, MI, 48823

<sup>2</sup> Department of Medicine, Division of Infectious Disease, Vanderbilt University Medical Center, Nashville, TN, 37232

<sup>3</sup> Department of Pathology, Microbiology, and Immunology, Vanderbilt University Medical Center, Nashville, TN, 37232

<sup>4</sup> Tennessee Valley Healthcare System, Department of Veterans Affairs, Nashville, TN

<sup>5</sup> Department of Medicine, Indiana University School of Medicine, Indianapolis, IN, 46202

<sup>6</sup> Department of Pathobiology and Diagnostic Investigation, Michigan State University, East Lansing, MI, 48823

\*co-corresponding authors

## 2 **ABSTRACT**

3 Group B *Streptococcus* (GBS) is a major cause of fetal and neonatal mortality worldwide. Many  
4 of the adverse effects associated with invasive GBS are associated with inflammation that leads  
5 to chorioamnionitis, preterm birth, sepsis, and meningitis; therefore, understanding bacterial  
6 factors that promote inflammation is of critical importance. Membrane vesicles (MVs), which  
7 are produced by many pathogenic and non-pathogenic bacteria, may modulate host inflammatory  
8 responses. In mice, GBS MVs injected intra-amniotically can induce preterm birth and fetal  
9 death. Although it is known that GBS MVs induce large-scale leukocyte recruitment into  
10 infected tissues, the immune effectors driving these responses are unclear. Here, we  
11 hypothesized that macrophages respond to GBS-derived MVs by producing proinflammatory  
12 cytokines and are recognized through one or more pattern recognition receptors. We show that  
13 THP-1 macrophage-like cells produce high levels of neutrophil- and monocyte-specific  
14 chemokines in response to MVs derived from different clinical isolates of GBS. Interleukin (IL)-  
15 1 $\beta$  was significantly upregulated in response to MVs, which was independent of NF- $\kappa$ B signaling  
16 but dependent on both caspase-1 and NLRP3. These data indicate that MVs contain one or more  
17 pathogen-associated molecular patterns that can be sensed by the immune system. Furthermore,  
18 this study identifies the NLRP3 inflammasome as a novel sensor of GBS MVs. Our data  
19 additionally indicate that MVs may serve as immune effectors that can be targeted for  
20 immunotherapeutics, particularly given that similar responses were observed across this subset of  
21 GBS isolates.

## 22 INTRODUCTION

23           Group B *Streptococcus* (GBS) is an opportunistic pathogen that colonizes the vaginal or  
24 rectal tract of ~30% of women (1). While maternal colonization is often asymptomatic, GBS can  
25 cause severe infections in pregnant women and neonates (1). Pregnancy- and neonatal-associated  
26 GBS infections are often characterized by pathologies exhibiting a high degree of inflammation.  
27 During pregnancy, this can present as placental villitis and preterm birth, whereas in neonates,  
28 GBS can cause meningitis and sepsis (2-4). Despite the high colonization frequencies in  
29 mothers, only a fraction of women and their neonates develop these threatening infections. The  
30 reasons for this discrepancy, however, are incompletely characterized.

31           We and others have postulated that strain variation contributes to the discrepancy in  
32 disease outcome. Indeed, specific phylogenetic lineages of GBS, which are defined by  
33 multilocus sequence typing (MLST) are more likely to cause neonatal infections (5-7). Notably,  
34 sequence type (ST)-17 strains are more commonly associated with invasive neonatal infections  
35 (5, 8, 9), whereas ST-1 strains are associated with invasive disease in adults (10). Conversely,  
36 ST-12 strains have been linked to asymptomatic maternal colonization (11). We demonstrated  
37 that ST-17 strains elicit stronger proinflammatory immune responses and persist longer inside  
38 macrophages than other strains (12, 13). Interestingly, we also found that ST-1 and ST-17 strains  
39 induce stronger activation of the proinflammatory transcription factor NF- $\kappa$ B compared to ST-12  
40 strains (13). While ST-17 strains were previously found to have unique virulence gene profiles  
41 relative to other lineages, the specific bacterial factor(s) promoting these altered inflammatory  
42 responses are not fully understood (14-16).

43           Recently it was reported that GBS produces membrane vesicles (MVs) that can induce  
44 substantial recruitment of neutrophils and lymphocytes into murine extraplacental membranes,  
45 which mimicked GBS-associated chorioamnionitis in humans (17, 18). In support of this finding,

46 GBS MVs were shown to induce production of the neutrophil chemokine CXCL1 in a murine  
47 model of *in utero* infection (17, 19), which has been shown in other GBS infection models (20,  
48 21). Further, we recently reported that GBS MV production varies in abundance and protein  
49 composition across STs (17, 19, 22). More specifically, several immunomodulatory virulence  
50 factors, including hyaluronidase, C5a peptidase, and sialidase were highly and differentially  
51 abundant across STs (22). Together these data indicate that MVs promote proinflammatory  
52 immune responses; however, no prior studies have comprehensively examined the mechanisms  
53 by which human leukocytes respond to GBS MVs.

54 As sentinel leukocytes at the maternal fetal interface, macrophages play an important role  
55 in shaping immune responses. At the maternal-fetal interface macrophages make up 20-30% of  
56 leukocytes (23) and play pivotal roles in fertility (24), placental function (25), and host-pathogen  
57 interactions at the maternal-fetal interface (26-28). The THP-1 monocytic leukemia cell line can  
58 be differentiated with phorbol esters into macrophage-liked cells (29) and serve as a model  
59 system to evaluate host responses to GBS (12, 30). Using this model, we previously showed that  
60 THP-1 cells produce high levels of proinflammatory cytokines in response to GBS. Interestingly,  
61 several cytokines displayed lineage-specific inflammatory responses, with ST-17 strains eliciting  
62 a more potent inflammatory response compared to other lineages (13). Here, we examined  
63 macrophage responses to GBS MVs isolated from a diverse set of strains and found that these  
64 MVs induce the production of proinflammatory cytokines and chemokines. We also identified  
65 NLRP3 as a sensor of GBS derived MVs. In all, this study has expanded our current  
66 understanding of how host cells respond to GBS MVs. Additionally, by identifying the pathways  
67 upregulated by MVs, we have identified the proinflammatory pathways and receptors that could  
68 be used as potential immunotherapeutic targets.

69

## 70 **METHODS**

### 71 **Bacterial Strains and Culture**

72 GBS strains GB0037 (GB37), GB0411 (GB411), GB0653 (GB653), and GB1455 were isolated  
73 as described previously (31, 32). The invasive isolates GB37, GB411, and GB1455, were  
74 isolated from the blood or cerebrospinal fluid of infants with early onset GBS disease (31), while  
75 the colonizing strain GB653 was isolated from vaginal/rectal swabs collected from an  
76 asymptotically colonized mother before childbirth (32). These isolates were previously  
77 characterized by MLST and capsular serotyping (9, 11). The GBS strains analyzed here represent  
78 colonizing and invasive isolates belonging to each of three common STs: ST-1 (GB37), ST-12  
79 (GB1455 and GB653), and ST-17 (GB411). Strains were cultured using Todd-Hewitt Broth  
80 (THB) or Todd-Hewitt Agar (THA) (BD Diagnostics, Franklin Lakes, New Jersey, USA)  
81 overnight at 37°C with 5% CO<sub>2</sub>.

82

### 83 **Membrane vesicle isolation**

84 MVs were isolated as previously described (22). Briefly, overnight THB cultures were  
85 diluted 1:50 into fresh broth and grown to late logarithmic phase (optical density (OD)<sub>600</sub> = 0.9).  
86 Cultures were centrifuged at 2000 x g for 20 minutes at 4°C. Supernatants were collected and re-  
87 centrifuged at 8500 x g for 15 minutes at 4°C, followed by filtration through a 0.22µm filter and  
88 concentration using Amicon Ultra-15 centrifugal filters (10 kDa cutoff) (MilliporeSigma,  
89 Burlington, MA, USA). Concentrated supernatants were subjected to ultracentrifugation for 2  
90 hours at 150,000 x g at 4°C. Pellets were resuspended in PBS and purified using qEV Single size  
91 exclusion columns (IZON Science, Christchurch, New Zealand) per the manufacturer's

92 instructions. MV fractions were collected and re-concentrated using the Amicon Ultra-4  
93 centrifugal filters (10 kDa cutoff) (MilliporeSigma, Burlington, Massachusetts, USA) and  
94 brought to a final volume of 100  $\mu$ L in PBS. MVs were aliquoted and stored at  $-80^{\circ}\text{C}$  until  
95 further use.

96

### 97 **Nanoparticle Tracking Analysis**

98 MVs were quantified via nanoparticle tracking analysis using a NanoSight NS300 (Malvern  
99 Panalytical Westborough, MA, USA) equipped with an automated syringe sampler as described  
100 previously (22, 33, 34). For each sample, MVs were diluted in PBS (1:100 – 1:1000) and  
101 injected with a flow rate of 50. Once loaded, five 20-second videos were recorded at a screen  
102 gain of 1 and camera level of 13, which were analyzed at a screen gain of 10 and a detection  
103 threshold of 4 after capture. Data were subsequently exported to a CSV file for analysis using the  
104 R package tidyNano (33).

105

### 106 **THP-1 Cell Culture**

107 THP-1 cells (TIB-202) were obtained through ATCC (Manassas, VA) and stored according to  
108 vendor guidelines (35). Briefly, cells were cultured in RPMI 1640 (Gibco, ThermoFisher,  
109 Waltham, MA) supplemented with L-Glutamine, 10% fetal bovine serum (FBS), and 1%  
110 antibiotic-antimycotic (100  $\mu\text{g}/\text{mL}$  Streptomycin, 0.25  $\mu\text{g}/\text{mL}$  Amphotericin B, & 100 U/mL  
111 Penicillin; Gibco, ThermoFisher, Waltham, MA) as previously described (12, 13). For  
112 experiments, THP-1 cells were only utilized until passage 10. When indicated, THP-1 monocytes  
113 were differentiated into macrophages using phorbol 12-myristate 13-acetate (PMA) as previously

114 described (12, 13). Cells were differentiated in RPMI (without phenol red) supplemented with L-  
115 Glutamine, 2% FBS and 100 nM PMA for 24 hours prior to experimentation (12, 13).

116

117 For experiments using GBS treated cells, THP-1 cells were washed twice with PBS prior to  
118 infection. The bacteria were resuspended in RPMI and added to the THP-1 cells at a multiplicity  
119 of infection (MOI) of 10 bacteria per cell. Cells were incubated for 1 hour and the media was  
120 subsequently aspirated. Cells were washed thrice with PBS and fresh RPMI with L-Glutamine  
121 (no phenol red) containing 2% FBS, 100 nM PMA, penicillin (5 µg/mL) and gentamicin  
122 (100µg/mL) was added (termed RPMI 2/0). Cells were incubated for an additional 24 hours. For  
123 MV treatment, cells were washed twice, and fresh RPMI 2/0 containing MVs at an MOI of 100  
124 MVs per differentiated macrophage was added and incubated for 25 hours. Cells were treated  
125 with LPS (1 µg/ml, clone L2654, Millipore Sigma, Burlington, MA) to serve as positive controls.  
126 At the end of each treatment period, supernatants were collected, centrifuged for 10 minutes at  
127 4000 rev/min at 4°C and aliquoted. Samples were stored at -80°C until used for downstream  
128 analysis.

129

### 130 **Cytokine and Cytotoxicity Analysis**

131 For semiquantitative analysis of cytokines in supernatants from THP-1 cultures, we employed a  
132 human cytokine antibody microarray (ab133998, Abcam, Cambridge, UK) according to  
133 manufacturer's instructions as previously described (13). Cells were seeded into 6-well plates at  
134 a density of  $4 \times 10^6$  per well and treated as described above. Membranes were imaged using an  
135 Amersham Imager 600 (GE Life Sciences), and densitometry was performed using ImageJ  
136 software. Cytokines falling above a fold change of 2 relative to mock treated were considered

137 upregulated and further analyzed. For subsequent analyses of cytokine production, caspase-1  
138 activation, and cell death, cells were seeded into 12-well plates at a density of  $2 \times 10^6$  cells per  
139 well and treated as described above. Cytokines with more than a 2-fold change relative to mock-  
140 treated cells were verified using a custom ProcartaPlex bead assay (ThermoFisher, Waltham,  
141 MA) as described by the manufacturer. These assays were read and analyzed using a Luminex  
142 200 and Luminex xPONENT v3.1 software, respectively (Luminex Corp., Austin, Texas).  
143 Cellular cytotoxicity was assessed using a CyQuant lactate dehydrogenase (LDH) assay  
144 (Invitrogen, Waltham, MA) per the manufacturer's instructions.

145

#### 146 **Immunofluorescence Staining and Microscopy Analysis**

147 THP-1 cells were differentiated into 4-well Nunc Lab-Tek II Chamber slides (ThermoFisher,  
148 Waltham, MA) at a density of  $10^5$  cells per well and differentiated as described above. Cells  
149 were treated with either MVs (MOI 100) or LPS (1  $\mu\text{g}/\text{mL}$ ) for 0.5 or 2 hours and stained for the  
150 NF- $\kappa$ B subunit p65 by immunofluorescence as described (36). Briefly, the cells were fixed using  
151 4% paraformaldehyde in PBS for 10 minutes, washed three times with ice cold PBS, and  
152 permeabilized for 10 minutes in 0.2% Triton-X in PBS. Cells were washed three more times in  
153 PBS and blocked in 10% goat serum/1% BSA/0.3% Tween in PBS for 20 minutes. Rabbit anti-  
154 NF- $\kappa$ B antibody (1:1600; clone D14E12; Cell Signaling Technology, Danvers, MA) was added  
155 to cells and incubated overnight at 4°C. Cells were washed three times and incubated with Alexa  
156 Fluor Goat anti-rabbit 546nm secondary antibody (10  $\mu\text{g}/\text{mL}$ ; Invitrogen, Waltham, MA) for 1  
157 hour, and washed again in PBS. Coverslips were mounted using Vectashield DAPI (Vector  
158 Laboratories, Inc., Burlingame, CA), and representative images were obtained using a Nikon



159 Eclipse Ti outfitted with a 20x plan fluor objective. Immunofluorescent microscopy was  
160 performed in biological triplicate for each timepoint and treatment.

161

### 162 **Caspase-1 Activity, Responses, and Inhibition**

163 After treatment of THP-1 cells, caspase-1 activity was quantified in supernatants using a  
164 commercially available assay (Caspase-GLO 1 Assay; Promega, Madison, WI) according to the  
165 manufacturer's instructions. Caspase-1 activity in supernatants was quantified using a GloMax  
166 Navigator (Promega, Madison, WI). To assess the impact of caspase-1 on MV-induced IL-1 $\beta$   
167 production, PMA-differentiated THP-1 cells were seeded into 12-well plates and pretreated with  
168 50 $\mu$ M of the caspase-1 inhibitor, Ac-YVAD-CHO (Cayman Chemical Company, Ann Arbor,  
169 MI), or 10  $\mu$ M of the NLRP3 inhibitor, MCC950 (Invitrogen, Waltham, MA), for 30 minutes.  
170 Cells were treated with either LPS or GBS as described above, and IL-1 $\beta$  concentrations were  
171 measured using a ProcartaPlex simplex assay (ThermoFisher, Waltham, MA).

172

### 173 **qPCR Analysis**

174 PMA-differentiated THP-1 cells, which were seeded in 12-well plates at a density of  $2 \times 10^6$   
175 cells per well, were left untreated or treated with either GBS bacteria, LPS, or MVs as described  
176 above. After 2 or 4 hours, supernatants were aspirated and cells were lysed by adding 1mL Trizol  
177 reagent (Invitrogen, Waltham, MA) and gentle scraping. Samples were stored at -20°C until  
178 RNA extraction was performed using Phase Lock gel heavy tubes per manufacturer's  
179 instructions (Quanta Bio, Beverly, MA). RNA was quantified using a Nanodrop 8000  
180 spectrophotometer (Thermo Scientific, Waltham, MA) and stored at -20 °C until use. Reverse  
181 transcription was performed on 0.5  $\mu$ g of total RNA using Quantitect Reverse Transcription Kit

182 (Qiagen, Hilden, Germany), and 2  $\mu$ L of the resulting cDNA was amplified by PCR using  
183 TaqMan Universal PCR Master Mix (Applied Biosystems, Waltham, MA) with Taqman probes  
184 specific for pro-IL-1 $\beta$  (Assay ID: Hs00174097\_m1) and GAPDH (Assay ID: Hs99999905\_m1).  
185 PCR was performed in a QuantStudio 5 real time thermal cycler for 35 cycles (Applied  
186 Biosystems, Waltham, MA).

187

### 188 **Data analysis**

189 Data analysis was performed using RStudio. Shapiro-Wilk tests were used to determine whether  
190 data followed a normal distribution. Normally distributed data were analyzed for significance  
191 using a two-way analysis of variance (ANOVA), followed by a Tukey HSD *post hoc* test.  
192 Alternatively, non-parametric data were analyzed using a Kruskal-Wallis test, followed by  
193 Dunn's *posthoc* test to test for differences between groups. Multiple hypothesis testing was  
194 corrected using Benjamini-Hochberg or Bonferroni correction when necessary. The analyses  
195 used for individual experiments are denoted in the figure legends for clarity.

196

197

198

199

200

201

202

203

204

## 205 RESULTS

### 206 *GBS MVs elicit proinflammatory cytokine responses*

207 We first sought to characterize the cytokine response elicited by MVs from a diverse set  
208 of GBS strains representing major STs in clinical circulation. Specifically, we characterized the  
209 cytokine response to MVs from an ST-1 strain (GB37), two ST-12 strains (GB653 and GB1455),  
210 and one ST-17 strain (GB411). Of note, GB37, GB1455, and GB411 were all isolated from  
211 infants with invasive infections, whereas GB653 was isolated from an asymptotically  
212 colonized mother. Human cytokine antibody microarrays revealed that MVs from GB411 and  
213 GB653 induced cytokine production from THP-1 macrophages. Of the 80 cytokines and  
214 chemokines assayed, 7 were upregulated at least 2-fold in comparison to the untreated cells  
215 (Supplemental Figure 1). Cytokines upregulated in responses to MVs included the monocyte and  
216 neutrophil chemokines, CCL1, CCL2, CXCL1, CCL20, the pyrogen IL-1 $\beta$ , and the  
217 proinflammatory cytokine IL-6 (Figure 1, Supplemental Figure 1). Several cytokines were also  
218 induced differentially between the two isolates: MVs from GB411 induced CXCL1, CCL1, and  
219 IL-1 $\beta$  more strongly than MVs from GB653 (Figure 1). However, the same trend was not  
220 observed when comparing cytokines between bacteria-treated THP-1 cells since GB411 and  
221 GB653 elicited similar cytokine responses for each of these targets (Figure 1).

222 To validate these differences in cytokine production, we used quantitative Luminex-  
223 based assays. Consistent with previous results (13), GBS induced a potent proinflammatory  
224 response relative to untreated controls (Supplemental Figure 2-3), though IL-6 production  
225 remained unchanged by MV exposures (Supplemental Figure 3). Moreover, the MVs induced  
226 CCL1, CCL20, CXCL10, CXCL1, and IL-1 $\beta$ , with no differences between the strains from  
227 which the MVs were derived (Figure 2). While CCL2 displayed an elevated response relative to

228 mock treatment, this induction was only significant for MVs produced by GB37, GB411, and  
229 GB1455.

230 Next, we assessed cytotoxicity for all strains examined above using a lactate  
231 dehydrogenase activity assay to ensure that these responses were not biased due to differential  
232 cell death. In these analyses, we found that bacteria induced moderate cytotoxicity that varied  
233 slightly across bacterial strains (Supplemental Figure 4). Notably, GB37 induced significantly  
234 more cytotoxicity than GB1455; however, this cytotoxicity was modest. Although low levels of  
235 cytotoxicity were observed during MV treatments, with an average of ~6%, the cytotoxicity  
236 levels did not vary across MVs produced by the four different GBS strains.

237

### 238 **Membrane vesicles induce caspase-1 activation**

239 Since IL-1 $\beta$  was significantly increased in response to all GBS MVs regardless of the  
240 strain, we sought to classify the inflammatory pathways that impact its production. Using the  
241 Caspase-GLO 1 assay, we detected caspase-1 activity in our untreated controls as well as our  
242 LPS-stimulated control, albeit at a substantially higher magnitude in our LPS control  
243 (Supplemental Figure 5). Detectable caspase-1 activity was also observed in response to MVs  
244 and the GBS strains, though some differences were noted. Compared to untreated controls, MVs  
245 from GB37, GB411, and GB1455 induced the most potent caspase-1 responses, providing  
246 confirmation that MVs were capable of inducing caspase-1 activity (Figure 3A, Supplemental  
247 Figure 5). Similarly, GB411 bacteria induced a higher degree of caspase-1 activation compared  
248 to untreated controls, which is consistent with our previous findings (Supplemental Figure 6).

249 Next, we sought to determine if alternative pathways may be contributing to the  
250 conversion of pro-IL-1 $\beta$  to mature active IL-1 $\beta$ . To assess this, we pretreated THP-1 cells with

251 the caspase-1 inhibitor Ac-YVAD-CHO prior to treatment with MVs or LPS for 25 hours. We  
252 found that LPS and untreated controls both produced lower amounts of IL-1 $\beta$  when pretreated  
253 with Ac-YVAD-CHO compared to the vehicle controls (83% and 90% reduction, respectively);  
254 Figure 3B). Furthermore, inhibition of caspase-1 by Ac-YVAD-CHO resulted in almost  
255 complete abrogation of MV-stimulated IL-1 $\beta$  secretion (91% reduction) compared to the vehicle  
256 control. Importantly, alterations in IL-1 $\beta$  production were not associated with cell death  
257 (Supplemental Figure 7). This finding therefore demonstrates that caspase-1 activation is  
258 necessary for the maturation of pro-IL-1 $\beta$  to mature IL-1 $\beta$  in response to GBS MVs, regardless  
259 of the strain type (Figure 3B).

260

#### 261 **NLRP3 is essential for MV mediated IL-1B secretion**

262 Having established that caspase-1 is required for IL-1 $\beta$  maturation, we next investigated  
263 the upstream sensor of MVs. Because GBS triggers inflammasome activation via a NLRP3-  
264 dependent mechanism, we assessed whether inhibition of NLRP3 could impact caspase-1  
265 activation in response to GBS MVs (37). Notably, inhibition of NLRP3 with the MCC950  
266 inhibitor prevented both MV- and GBS-induced caspase-1 activity (Figure 4A and Supplemental  
267 Figure 8). We observed a similar trend in our control cells, demonstrating some baseline  
268 inflammasome activity in THP-1 cells; however, the magnitude of inflammasome activation was  
269 lower in control groups (Figure 4A). Inhibition of NLRP3 also reduced cytotoxicity for both the  
270 GBS bacteria- and MV-treated cells; however, this result was not observed for our untreated  
271 controls (Figure 4B).

272 Using a similar approach, we also assessed whether NLRP3 impacted secretion of IL-1 $\beta$   
273 from THP-1 cells. In these experiments, we found that inhibition of NLRP3 signaling

274 significantly decreased IL-1 $\beta$  secretion in both the media and LPS controls relative to the vehicle  
275 controls (Figure 4C). While the decrease was significant in both groups, the effect was lower for  
276 the untreated controls. Moreover, NLRP3 inhibition reduced IL-1 $\beta$  secretion in response to both  
277 GBS and the MVs demonstrating that MV-induced IL-1 $\beta$  requires NLRP3 (Figure 4C).

278

### 279 **Membrane vesicles do not trigger transcription activation of pro-IL-1B**

280 We next assessed whether the high levels of IL-1 $\beta$  produced in response to GBS MVs  
281 were due to the release of existing pools of pro-IL-1 $\beta$ , or if MVs could directly induce  
282 transcription of pro-IL-1 $\beta$ . Using RT-qPCR analysis, we observed no significant increase in pro-  
283 IL-1 $\beta$  gene expression relative to untreated cells for LPS, MV, or bacteria treated THP-1 cells at  
284 2 hours post infection (Figure 5A). At 4 hours post infection, however, LPS induced a significant  
285 increase in pro-IL-1 $\beta$  gene expression relative to untreated cells, but no similar increases were  
286 observed in response to MVs or GBS (Figure 5A). Using immunofluorescence, we similarly  
287 found that while LPS rapidly induced the translocation of the NF- $\kappa$ B subunit p65, neither  
288 untreated nor MV treated THP-1s induced NF- $\kappa$ B translocation. Notably, MVs induced no NF-  
289  $\kappa$ B translocation in response to MVs after a 2-hour exposure (Figure 5B). Similar results were  
290 observed at 30 minutes post exposure (Supplemental Figure 9). Together, these data indicate that  
291 MVs do not induce a largescale alteration in pro-IL-1 $\beta$  gene expression or NF- $\kappa$ B activation,  
292 suggesting that elevated IL-1 $\beta$  secretion is likely due to post-translational regulation.

293

294

295

296

297 **DISCUSSION**

298 Previous studies demonstrated that *in utero* exposure to GBS MVs induced recruitment of  
299 neutrophils and lymphocytes into the gestational membranes (17), while MVs induced neutrophil  
300 recruitment to the lung in a neonatal sepsis model (19); however, the signals that perpetuate the  
301 influx of leukocytes remains unclear. Herein, we have demonstrated that MVs induce expression  
302 of proinflammatory cytokines and chemokines in human macrophages *in vitro*, which likely  
303 contribute to the inflammatory infiltrate observed *in vivo* (17, 19). Additionally, we found that  
304 MVs induce the production of IL-1 $\beta$  by activating pro-IL-1 $\beta$  maturation in an NLRP3 and  
305 caspase-1 dependent manner, but independently of NF- $\kappa$ B signaling.

306 By expanding our current understanding of the cytokine responses towards GBS derived  
307 MVs, we have identified the modulators that likely impact the adverse pathologies observed *in*  
308 *vivo*. A previous study demonstrated that the murine chemokine KC, known as CXCL1 in  
309 humans, was upregulated in response to GBS MVs (17). In support of these findings, we  
310 demonstrate that production of CXCL1 and many additional chemokines are upregulated in  
311 human macrophages following challenge with GBS MVs. Notably, CCL1, CCL20, CXCL1, and  
312 CXCL10 were all significantly upregulated in response to MVs from four clinical strains.  
313 Similarly, the chemokine CCL2 was significantly elevated in response to three of the clinical  
314 strains we examined. These chemokines are critical for recruitment of leukocytes to sites of  
315 infection, with varying target cell specificities. CXCL1 and CCL20, for example, attract  
316 neutrophils (38-40), whereas CCL1 and CCL2 attract monocytes and macrophages (41, 42).  
317 Additionally, CCL20 and CXCL10 recruit lymphocytes (40, 43). Unsurprisingly, many of the  
318 cytokines have been implicated in GBS-associated disease. For example, CCL20 is upregulated  
319 during infection at the blood brain barrier (44). Similarly, CCL2 has been shown to be strongly

320 upregulated during GBS sepsis cases (45). Taken together these data indicate that GBS MVs  
321 serve as a critical initiator of disease associated cytokine responses.

322 Another cytokine that was significantly upregulated in response to MVs was the pyrogen  
323 IL-1 $\beta$ , which plays a critical role in the host defense to GBS infections by promoting production  
324 of additional neutrophil specific chemokines (20, 46). Although IL-1 $\beta$  does not have direct  
325 chemoattractant activity, IL-1 $\beta$  signaling does impact the production of CXCL1 in GBS  
326 infections (20). In fact, IL1R knockout mice display reduced neutrophil recruitment and  
327 significant increases in mortality when challenged with GBS (46). Given the abundant  
328 recruitment of neutrophils and lymphocytes into MV challenged tissues (17), these data provide  
329 critical insights into the mechanisms driving this leukocyte infiltration. Although we and others  
330 have shown strain variation in IL-1 $\beta$  production in response to whole bacteria (13, 47), here we  
331 found that MVs consistently elicited a consistent level of IL-1 $\beta$  from human macrophages,  
332 suggesting that it may serve as an important biomarker or possibly a therapeutic target.

333 Previous studies have highlighted the signaling pathways involved in producing mature  
334 IL-1 $\beta$ . Notably, high levels of this cytokine were only produced when both TLR (toll-like  
335 receptor) signaling and inflammasome activation occurred (48). TLR signaling occurs when  
336 pathogen-associated molecular patterns (PAMPs) engage their cognate receptor (49, 50), which  
337 results in the induction of proinflammatory gene expression, including the inactive form of this  
338 cytokine, pro-IL-1 $\beta$  (50). Canonically, the induction of pro-IL-1 $\beta$  gene expression depends on  
339 translocation of the transcription factor NF- $\kappa$ B, into the nucleus (51).

340 For pro-IL-1 $\beta$  to be secreted in its mature, active form, a second signal is required. This  
341 signal is typically in the form of a danger associated molecular pattern (DAMPs), such as a  
342 change in membrane potential due to membrane damage (52, 53). DAMPs are sensed by NLRPs



343 (Nucleotide-binding oligomerization domain, Leucine rich Repeat and Pyrin domain-containing  
344 receptors) (52, 54). Once sensed, NLRPs oligomerize with other subunits, forming the  
345 inflammasome, (52, 55, 56) which cleaves pro-caspase-1 into its mature, active form (56, 57).  
346 Active caspase-1 then cleaves pro-IL-1 $\beta$ , triggering its release (57). This concerted process  
347 results in release of stored pools of pro-IL-1 $\beta$ , allowing for rapid immune activation.

348 Notably, we demonstrate that GBS MVs trigger caspase-1 activation in human  
349 macrophages and that the secretion of IL-1 $\beta$  is dependent on caspase-1 activation. Our findings  
350 further indicate that MVs do not trigger expression of pro-IL-1 $\beta$  or activation of NF- $\kappa$ B,  
351 suggesting that IL-1 $\beta$  production in response to MVs is largely due to post-transcriptional  
352 regulatory mechanisms. Interestingly, we also found that caspase-1 activation is ablated in the  
353 absence of NLRP3, suggesting that NLRP3 is a sensor of GBS MVs. While previous reports  
354 have demonstrated that GBS induces IL-1 $\beta$  production in a NLRP3-dependent manner, this is the  
355 first study to demonstrate that GBS MVs contribute to this response (28, 37, 58). Furthermore,  
356 we are not aware of any other studies that have identified a pattern recognition receptor capable  
357 of sensing GBS MVs. This newfound information may allow for the development of receptor  
358 antagonist therapies targeting the NLRP3 dependent recognition of GBS MVs, which could  
359 prevent host inflammation and subsequent adverse pregnancy outcomes.

360 Our data also indicate that inhibition of the NLRP3 inflammasome reduces MV-induced  
361 cytotoxicity of macrophages *in vitro*. Several studies have shown that GBS virulence factors,  
362 such as hemolysin can induce NLRP3-dependent pyroptosis (37, 58-60). Other studies indicate  
363 that GBS mediated pyroptosis is mediated by the activation of the pore forming mediator of  
364 pyroptosis, gasdermin D (61, 62). In our examination of THP-1 macrophages, both the MVs and  
365 bacteria mediated a modest amount of cell death, which was dependent on the NLRP3

366 inflammasome, suggesting that MVs can induce pyroptosis, which could suggest gasdermin D  
367 activation. While further studies are needed to confirm this hypothesis, the high levels of IL-1 $\beta$   
368 production together with NLRP3 mediated cell death indicate that MVs may be partly  
369 responsible for GBS-mediated pyroptosis.

370 Our analyses also suggest that MVs do not induce pro-IL-1 $\beta$  gene expression. Indeed,  
371 while LPS induced a potent upregulation of pro-IL-1 $\beta$  by 4 hours post-exposure, we observed no  
372 upregulation of pro-IL-1 $\beta$  in response to MVs or bacteria at either timepoint. Additionally, this  
373 lack of induction correlated with the activation of NF- $\kappa$ B signaling, which suggests the  
374 following: 1) MVs do not overwhelmingly induce the expression of pro-IL-1 $\beta$ ; and 2) the  
375 upregulation of IL-1 $\beta$  signaling is likely due to the activation of inflammasome signaling in  
376 primed macrophages. Taken together, these data indicate that GBS MVs induce the production  
377 of IL-1 $\beta$  in primed macrophages, which is likely a conserved feature of GBS MVs.

378 A prior study demonstrated that GBS MVs contain active hemolysin and that MV-  
379 associated hemolysin exacerbates neonatal sepsis *in vivo* (19). Although it was suggested that  
380 GBS-mediated caspase-1 induction requires GBS hemolysin (37), our data indicate that MVs  
381 from a non-hemolytic strain of GBS (GB0037) still induce a robust IL-1 $\beta$  response and activate  
382 caspase-1 (63). This finding indicates that other factors associated with MVs also induce  
383 caspase-1 activation. Indeed, use of proteomics in our prior study found that MVs of different  
384 genetic backgrounds contained multiple virulence factors that have been linked to inflammatory  
385 responses previously (22). Several factors known to promote immune evasion, such as  
386 hyaluronidase, sialidase, and C5a peptidase, were present in GBS MVs at variable levels across  
387 diverse phylogenetic backgrounds (22). While these factors can diminish host sensing of GBS,  
388 other MV-derived factors likely promote these inflammatory responses. Nonetheless, future

389 studies are required to classify the role that these other factors play in activating these signaling  
390 cascades.

391         Despite advancing our current understanding of the host response elicited towards GBS  
392 MVs, it is important to recognize the limitations of our study. Although no strain-specific  
393 immune responses towards GBS MVs were observed, we only examined 4 distinct clinical  
394 isolates that could have limited our ability to detect differences. Furthermore, our cytokine  
395 analysis was limited to those included in the antibody microarrays; hence, it is likely that other  
396 responses may also be important. Although our results are consistent with previous reports  
397 regarding the host response to GBS MVs (17, 19), it is possible that our system lacks the  
398 appropriate complexity to fully model the host response to GBS MVs. Indeed, although THP-1  
399 cells have been shown to largely recapitulate the responses elicited from peripheral blood  
400 mononuclear cells, the magnitude of their responses can vary between these two systems (64).  
401 Furthermore, the use of cells in monoculture does not capture the complexity of the host  
402 responses observed *in vivo*. Therefore, future studies using alternative model systems are  
403 warranted.

404         Overall, data from this study enhance our understanding of how GBS MVs promote both  
405 adverse pregnancy and neonatal infection outcomes (Figure 6). It has been established that GBS  
406 MVs promote adverse outcomes partly by enhancing neutrophil recruitment (17, 19). In  
407 conditions such as chorioamnionitis, we suggest that the sensing of MVs by macrophages may  
408 promote proinflammatory immune signaling. Consistent with these findings, we have  
409 demonstrated that MVs promote the release of many neutrophil recruiting chemokines as well as  
410 the pyrogen IL-1 $\beta$ , which are important for neutrophil recruitment that promote tissue damage  
411 via net-osis (20, 40, 65, 66). We also demonstrate that the MV-mediated induction of IL-1 $\beta$  is

412 dependent on caspase-1 activation, which further promotes a proinflammatory environment.  
413 Through both direct and indirect tissue damage, MVs likely play a role in weakening gestational  
414 membranes, inducing chorioamnionitis, and promoting preterm labor due to enhanced induction  
415 of these inflammatory responses (Figure 6). Collectively, these findings expand our  
416 understanding of how the immune system respond to these bacterial components that contain  
417 important virulence factors capable of initiating an inflammatory response. While the specific  
418 PAMPs and DAMPs contained in MVs are not known, this study provides a foundation for  
419 future studies aiming to classify the specific factors within MVs that trigger these responses.

420         These data illustrate that GBS MVs can induce potent proinflammatory cytokine  
421 responses, which is due in part to the activation of the NLRP3 inflammasome. This study  
422 advances our understanding of how GBS MVs interact with the host, by identifying the cytokine  
423 response towards GBS MVs as well as by identifying NLRP3 as a sensor of MVs. Furthermore,  
424 because these cytokine responses are largely conserved across genetically distinct clinical GBS  
425 isolates, these responses may represent important targets for immunotherapy or as biomarkers for  
426 disease status. Taken together, this study has provided mechanistic insight into the immune  
427 response elicited towards GBS MVs.

428

429

430

431

432

433

434

435 **Funding information**

436 This work was funded by the National Institutes of Health (NIH; AI154192 to S.D.M and  
437 M.G.P.) with additional support provided by AI134036 to D.M.A, HD090061 to J.A.G. and  
438 BX005352 from the Office of Research, Department of Veterans Affairs. Graduate student  
439 support for C.R.M. was provided by the Reproductive and Developmental Science Training  
440 Program funded by the NIH (T32 HDO87166) as well as the Eleanor L. Gilmore Endowed  
441 Excellence Award.

442

443 **Acknowledgments**

444 We would like to thank Dr. H. Dele Davies for sharing the bacterial strains and Drs. Sean L.  
445 Nguyen and Soo H. Ahn for helpful conversations and assistance with data analysis. We would  
446 also like to thank Dr. Matt Bernard for his assistance with Luminex analyses.

447

448 **Conflict of interest statement**

449 The authors declare that the research was conducted in the absence of any commercial or  
450 financial relationships that could be construed as a potential conflict of interest.

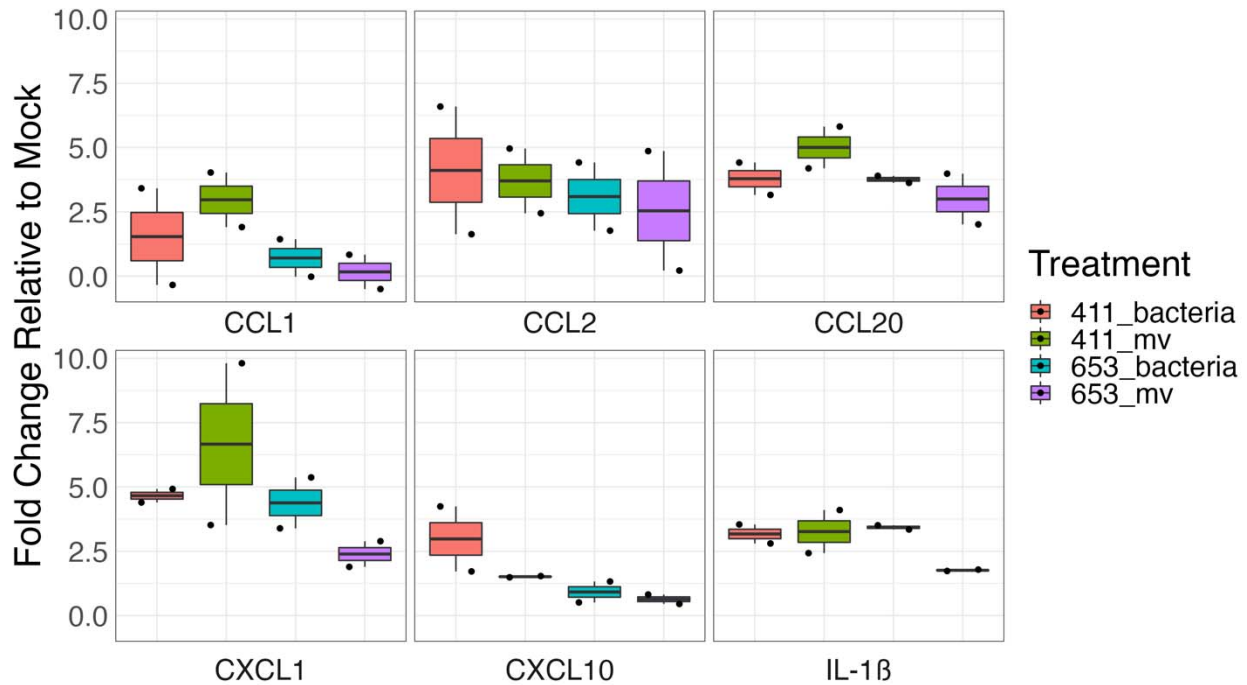
451

452 **Author Contributions Statement**

453 CRM, MGP, and SDM designed the study; CRM performed the laboratory work and conducted  
454 the analysis; MGP, SDM, DMA, and JGA provided institutional support, guidance and  
455 resources, and CRM drafted the manuscript. All authors contributed to and approved of the  
456 manuscript content.

457

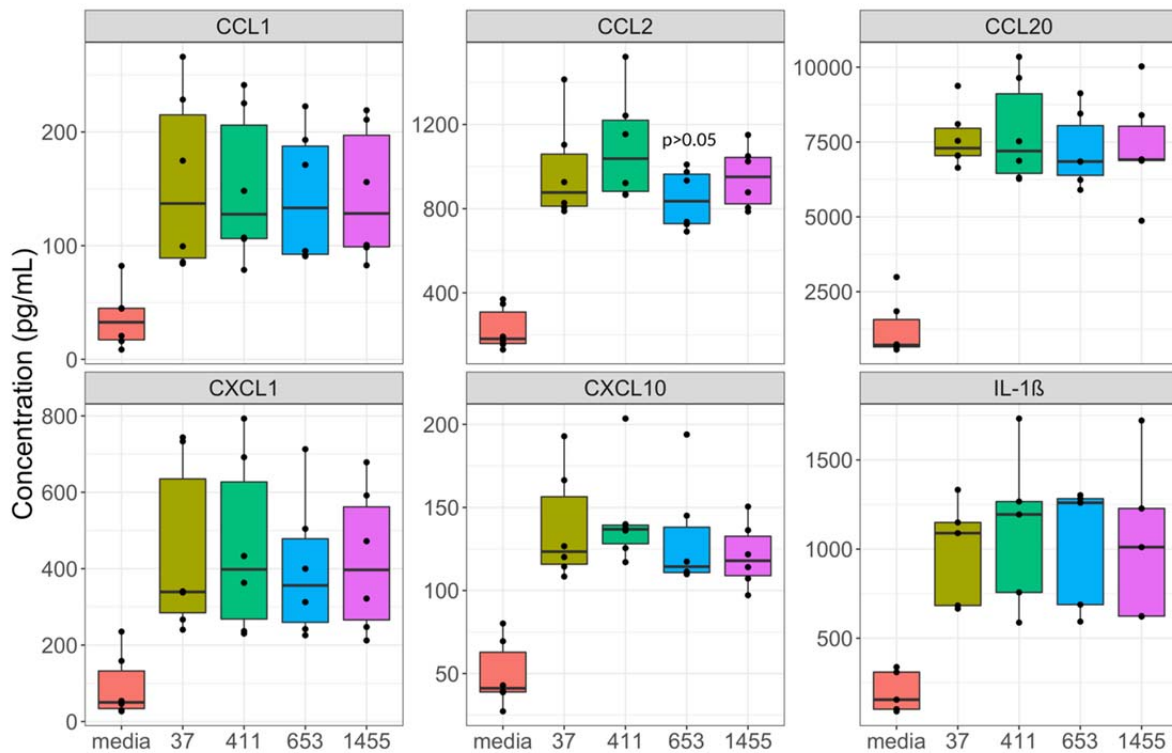
458 **Figures:**



459 **Figure 1: Human antibody cytokine microarray reveals highly upregulated cytokines in**  
460 **response to GBS and GBS MVs.**

461 Human cytokine antibody microarrays (Abcam) were probed with supernatants from untreated,  
462 bacteria-treated, or MV-treated THP-1-derived macrophages. Membrane densitometry was  
463 assessed using ImageJ software. The bacterial strains used are an invasive ST-17 strain (GB411)  
464 and a colonizing ST-12 strain (GB653). Shown here are hits of interest that displayed greater  
465 than 2-fold change (FC) induction relative to untreated controls in at least one group. Black dots  
466 indicate a single biological replicate. n = 2/treatment.

467  
468  
469  
470  
471



472

473 **Figure 2: MVs induce proinflammatory cytokine and chemokine responses**

474 Supernatants from THP-1 derived macrophages which were untreated or treated with MVs (MOI

475 100) for 25 hours were assessed for cytokine production using ProcartaPlex multiplex or

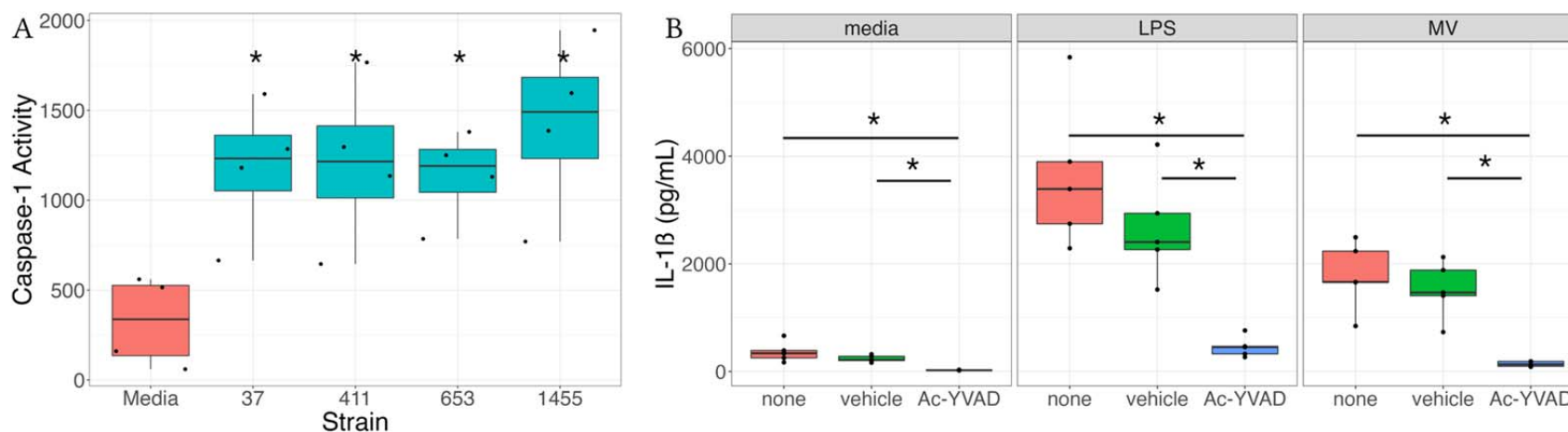
476 singleplex (IL-1B) bead-based assays. Individual black dots indicate a single biological replicate

477 (n = 5-6 for each group). Statistics were determined using either an ANOVA with a Tukey HSD

478 post hoc or a Kruskal Wallis test with a Dunn Test post hoc when appropriate. All comparisons

479 to mock treatment were significant (p<0.05) unless noted with a specific p-value.

480



481  
482

**Figure 3: Caspase-1 is critical for the host response to GBS MVs**

483

484

485

486

487

488

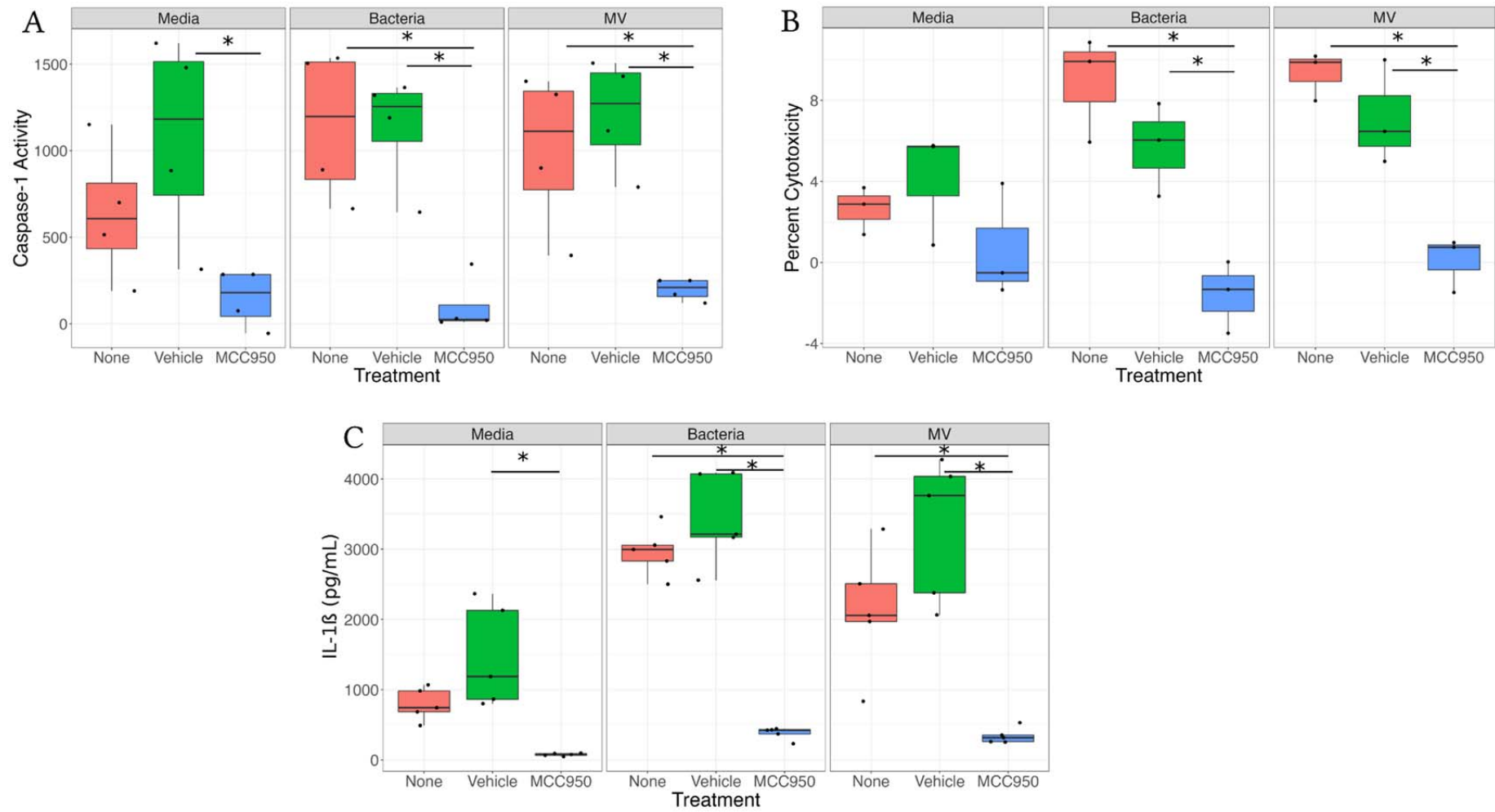
489

490

491

A.) THP-1 derived macrophages were unstimulated or treated with MVs for 25 hours. Supernatants were then assessed for caspase-1 activity using a caspase-1 GLO assay. Relative light units (RLU) were obtained from a GLO Max Navigator. Data represent the amount of caspase-1 activity (caspase-1 activity = (RLU GLO) - (RLU AC)) from paired samples. B.) THP-1 derived macrophages were pre-treated media, ethanol (vehicle), or Ac-YVAD-CHO for 30 minutes prior to stimulation with LPS, media, or MVs for 25 hours. Supernatants were then assessed for IL-1 $\beta$  concentration using ProcartaPlex bead-based assays. Individual black dots indicate a single biological replicate (n = 4 for each group). Statistical significance is defined as p<0.05 as calculated by ANOVA with a Tukey post-hoc and indicated by (\*).





492

493

494

495

496

497 **Figure 4: Inhibition of NLRP3 Ablates Caspase-1 Activity in Response to MVs**

498 THP-1s were treated with the NLRP3 inhibitor MCC950 or DMSO for 30 minutes prior to treatment with bacteria, MVs, or media for  
499 25 hours. A.) Caspase-1 activity was determined using the Caspase-1 GLO assay. Caspase 1 activity = ((GLO reagent) – (Ac-YVAD-  
500 CHO + GLO Reagent)). Individual points represent individual biological replicates (n = 4 each group). B.) Supernatants were assessed  
501 for cytotoxicity using the CyQuant LDH Assay. Individual black dots indicate a single biological replicate (n = 3 for each group). C.)  
502 IL-1 $\beta$  contained in supernatants was quantified using ProcartaPlex IL-1 $\beta$  single plex assays. Individual points represent individual  
503 biological replicates (n = 5 each group). Statistics were determined using an ANOVA with a Tukey's HSD post-hoc test. Significance  
504 was defined as p<0.05 and denoted with an (\*).

505

506

507

508

509

510

511

512

513

514

515

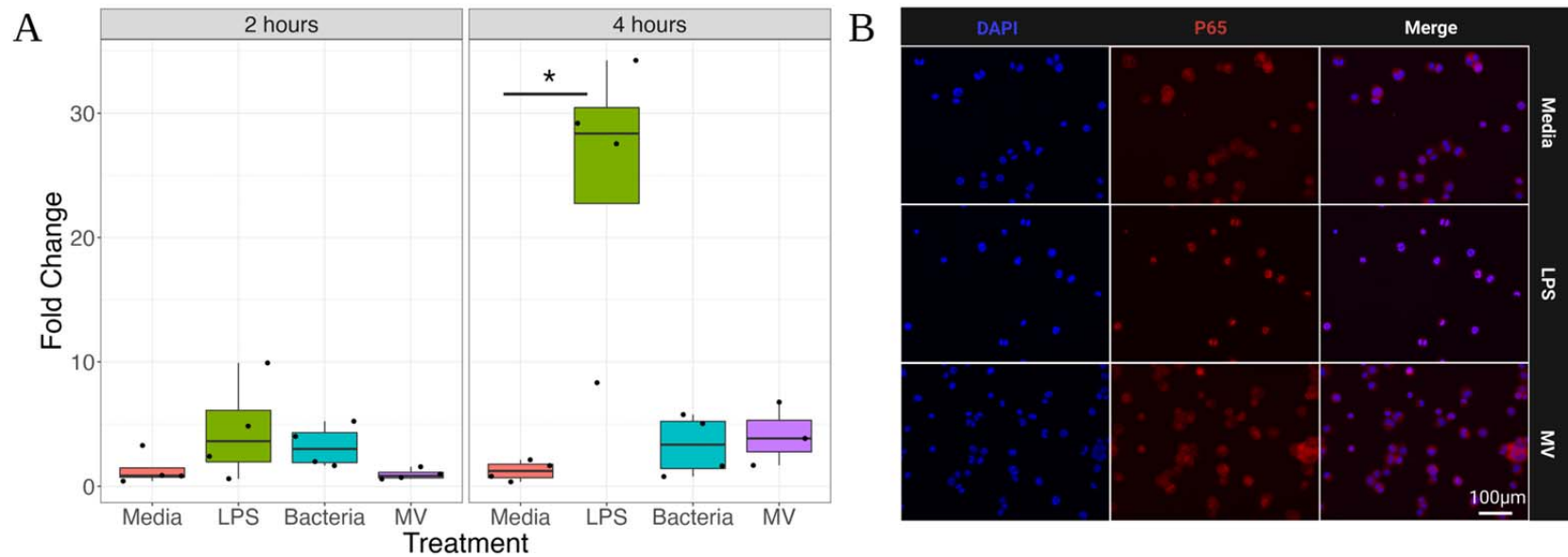
516

517

518

519

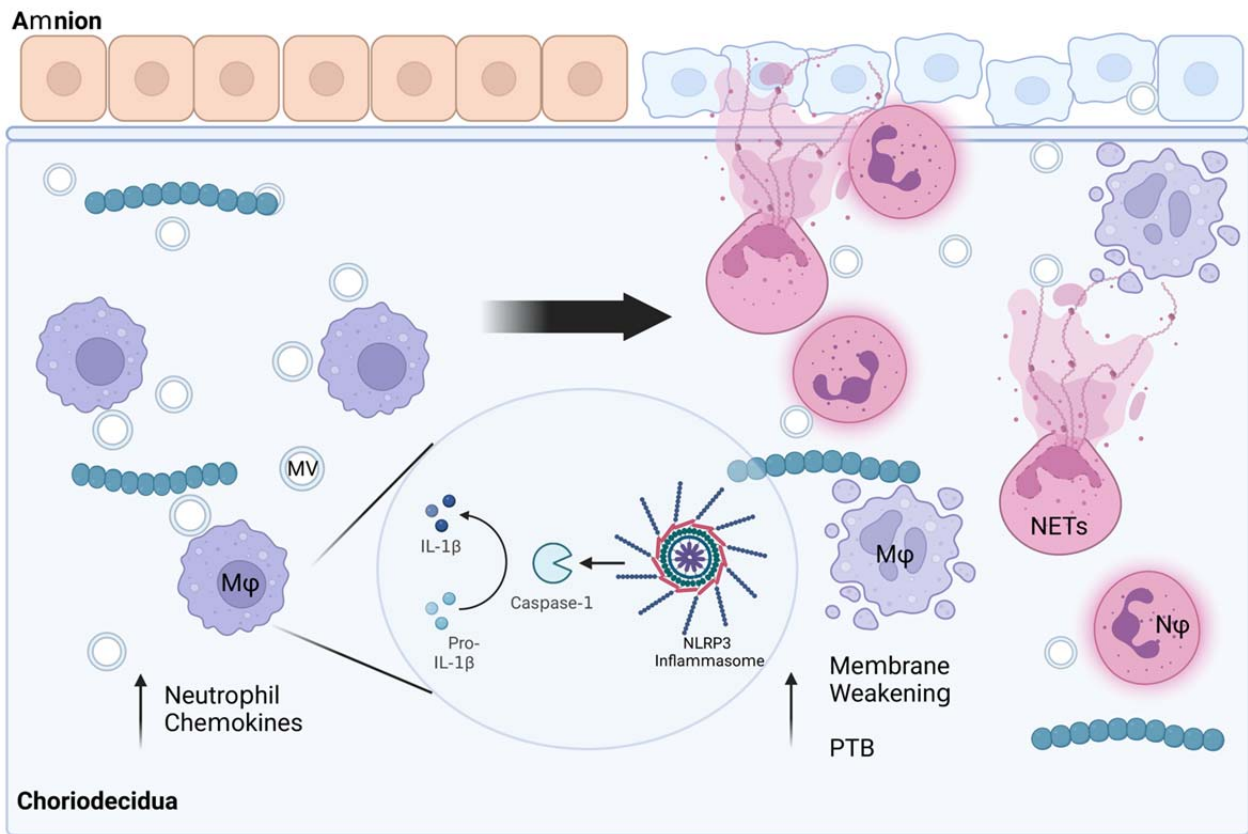
520  
521



522  
523  
524

**Figure 5: MVs do not prime human macrophages.**

525 A.) Expression of pro-IL-1 $\beta$  mRNA from THP-1s treated with bacteria, MVs, LPS, or media was quantified using Taqman probes at 2  
526 and 4 hours after treatment. Fold change values were calculated relative to respective media controls. Each individual dot represents a  
527 single biological replicate (n = 4/group). Statistics are calculated using a t-test or Wilcoxon test when appropriate. Significance was  
528 defined as p<0.05 and denoted by (\*). B.) Differentiated THP-1 derived macrophages were untreated or treated with LPS or MVs for 2  
529 hours prior to fixation and immunofluorescence staining for NF-kB subunit p65 (stained red). Nuclei are stained using DAPI (blue).  
530 Shown here are representative images (n = 5) taken at 40x magnification.



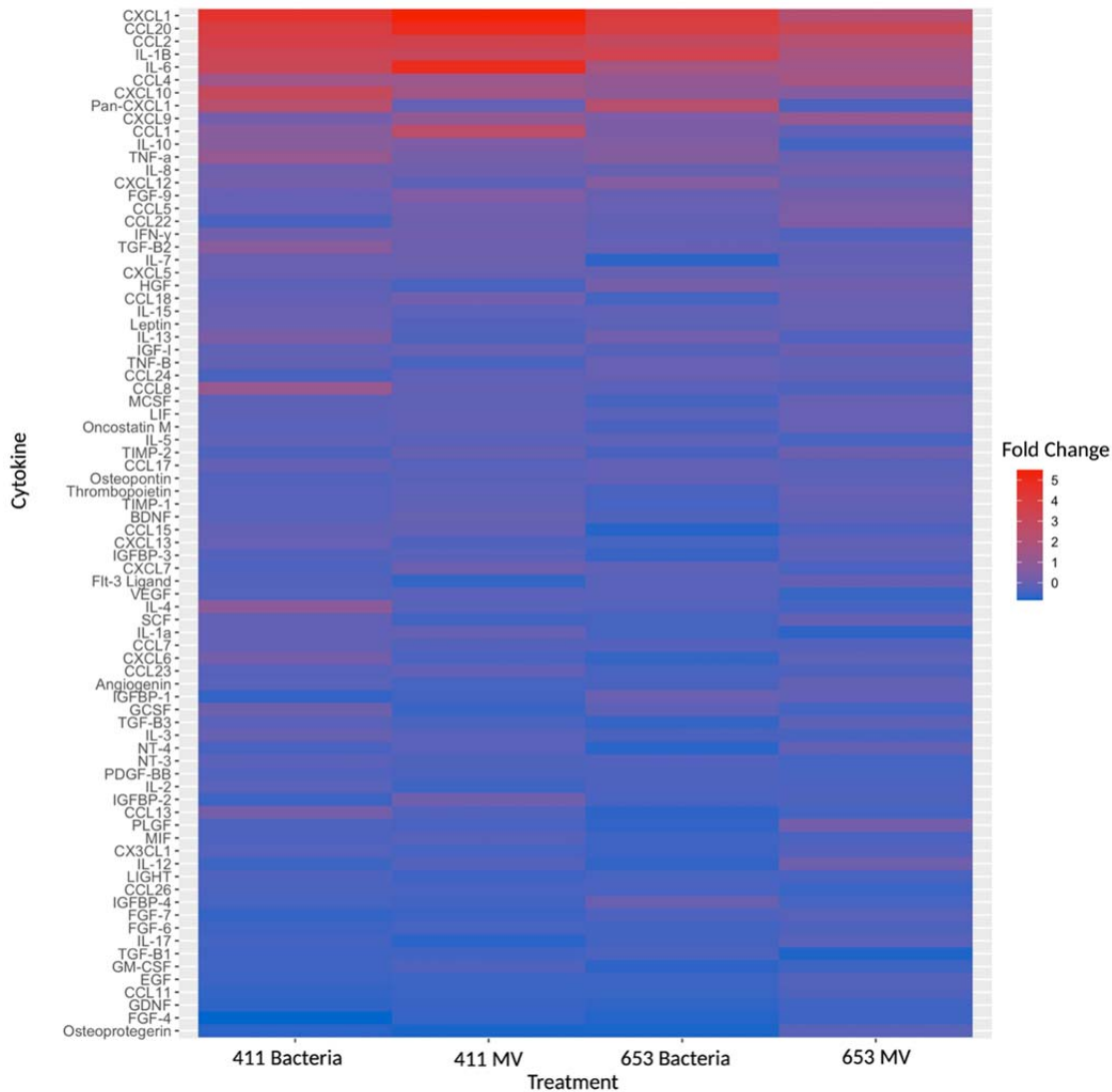
531  
532

### 533 **Figure 6: Model of GBS Mediated Chorioamnionitis**

534 GBS is a frequent cause of chorioamnionitis. As sentinel cells at the maternal-fetal interface,  
535 macrophages play a critical role in shaping how inflammatory responses are initiated. We show  
536 here that macrophages respond to MVs by releasing proinflammatory cytokines and chemokines,  
537 many of which recruit neutrophils to the site of infection. Additionally, we show that MVs  
538 activate the NLRP3 inflammasome, triggering release of the pyrogen IL-1 $\beta$ . Together these  
539 processes promote an influx of neutrophils and leukocytes into the site of infection. In cases such  
540 as chorioamnionitis, neutrophils undergo processes including NET-osis, which promote tissue  
541 weakening and subsequent preterm birth. Taken together these findings demonstrate  
542 mechanistically how MVs may promote preterm birth and chorioamnionitis *in vivo*.

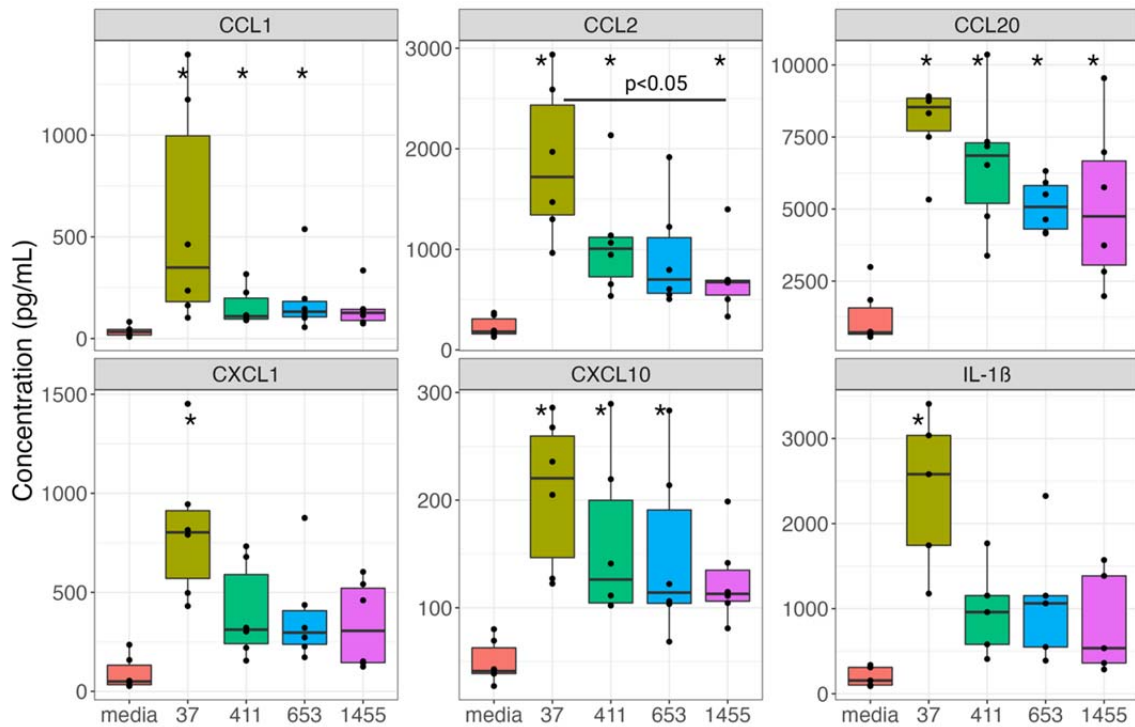
543

544  
545



546 **Supplemental Figure 1: Profiling of cytokine responses elicited towards MVs**

547 THP-1s were treated with bacteria (multiplicity of infection (MOI) = 10) or MVs (MOI 100) for  
548 25 hours prior to supernatant collection. Cytokine production was analyzed using a human  
549 cytokine antibody microarray (Abcam). Shown here is semi-quantitative densitometry analysis  
550 (ImageJ) of cytokine production for all 80 cytokines examined. Color denotes fold change  
551 relative to untreated controls. All groups were performed in biological duplicate. Boxes indicate  
552 mean fold change for each condition.



553  
554

555 **Supplemental Figure 2: Bacteria elicit proinflammatory immune responses from THP-1**  
556 **macrophages.**

557

558 Supernatants from THP-1 derived macrophages, which were untreated or treated with bacteria

559 (MOI 10) for 25 hours were assessed for cytokine production using ProcartaPlex multiplex bead-

560 based assays. Each black dot indicates a single biological replicate (n = 5-6 for each group). Data

561 were analyzed by one-way ANOVA with a Tukey HSD post hoc test, or for non-parametric data,

562 a Kruskal Wallis test with a Dunn Test post hoc test. Comparisons with  $p < 0.05$  relative to

563 untreated are denoted with (\*). Significant differences between strains are denoted with a

564 specific p-value.

565

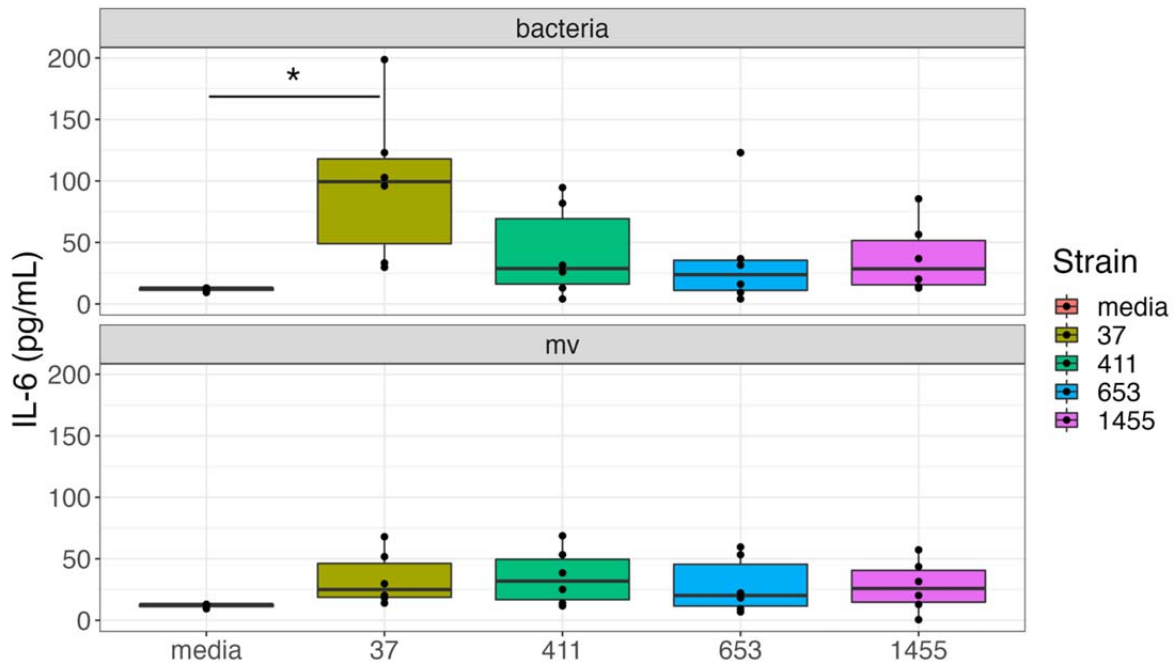
566

567

568

569

570  
571

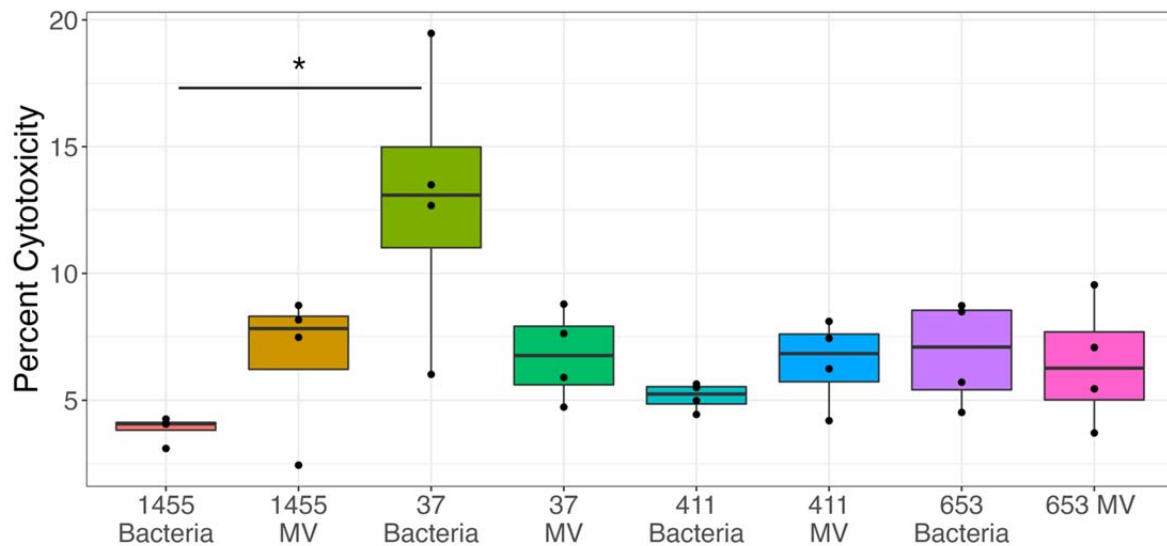


572  
573 **Supplemental Figure 3: IL-6 is not produced in response to GBS MVs**

574 Supernatants from unstimulated or MV-treated THP-1 derived macrophages were assessed for  
575 IL-6 using ProcartaPlex multiplex bead-based assays. Individual black dots indicate a single  
576 biological replicate (n = 5-6 for each group). Statistics were determined by one-way ANOVA  
577 with a Tukey HSD post hoc, or for non-parametric data, a Kruskal Wallis test with a Dunn post  
578 hoc test. Significantly different comparison between groups (P-value < 0.05) are denoted with  
579 (\*).

580  
581  
582  
583  
584  
585  
586

587  
588  
589  
590  
591  
592  
593



594  
595

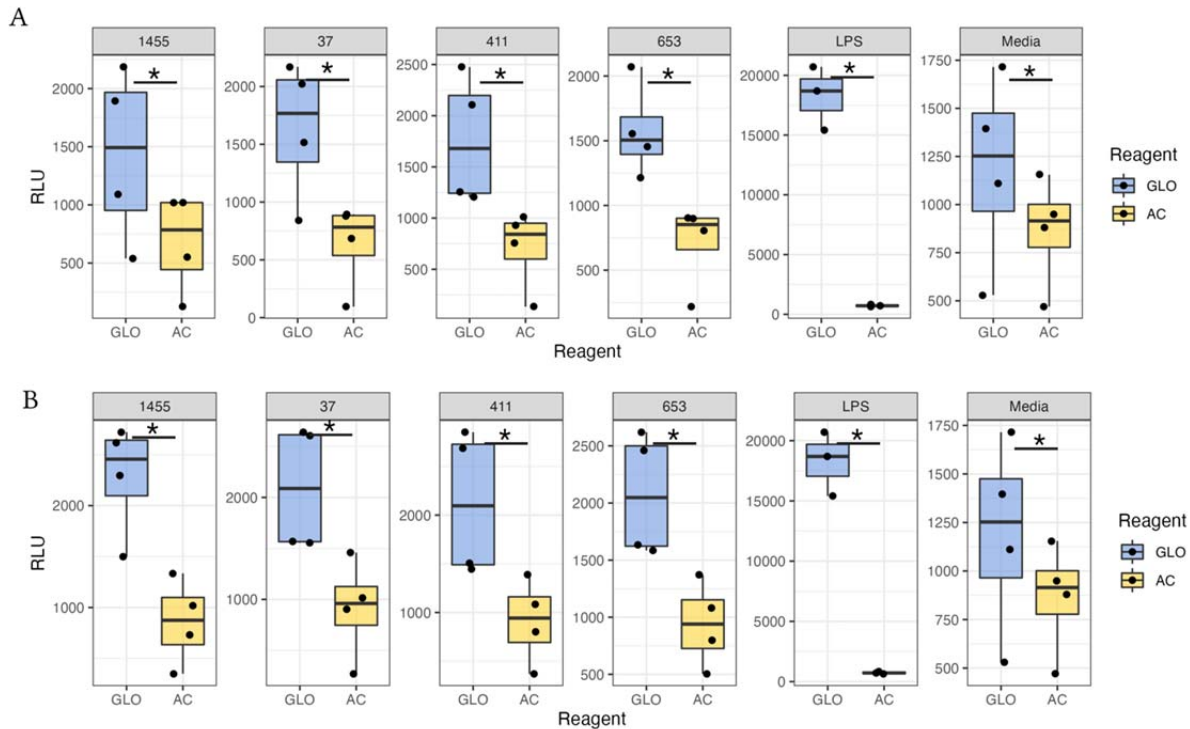
#### Supplemental Figure 4: MVs induce a low amount of cell death in THP-1s

596 THP-1 derived macrophages were unstimulated or treated with MVs for 25 hours.  
597 Supernatants were assessed for cytotoxicity using the CyQuant LDH Assay. Percent Cytotoxicity  
598 is expressed as a percentage relative to untreated cells. Each black dot represents a single  
599 biological replicate (n = 4 /group). Data were analyzed using either a one-way ANOVA with a  
600 Tukey HSD post hoc test (MV treated groups), or a Kruskal Wallis test with a Dunn Test post  
601 hoc (Bacteria-treated groups). Significantly different comparison within groups (P-value < 0.05)  
602 are denoted with (\*). All other comparisons were not significantly different.

603  
604  
605  
606  
607  
608



609



610

### 611 **Supplemental Figure 5: MVs induce caspase-1 activity**

612 Supernatants from THP-1 derived macrophages which were unstimulated or treated with

613 bacteria, MVs for 25 hours. Alternatively, cells were stimulated with LPS for 2 hours.

614 Supernatants were then assessed for caspase-1 activity using a caspase-1 GLO assay. A.)

615 Activity from THP-1s treated with bacteria. B.) Activity from THP-1s treated with MVs.

616 Relative light units (RLU) were determined using a GLO Max Navigator. Individual black dots

617 indicate a single biological replicate (n = 3-4 for each group). Statistics were determined using a

618 two-sided, paired t-test. P-value < 0.05 relative to mock treatment is denoted with a (\*).

619

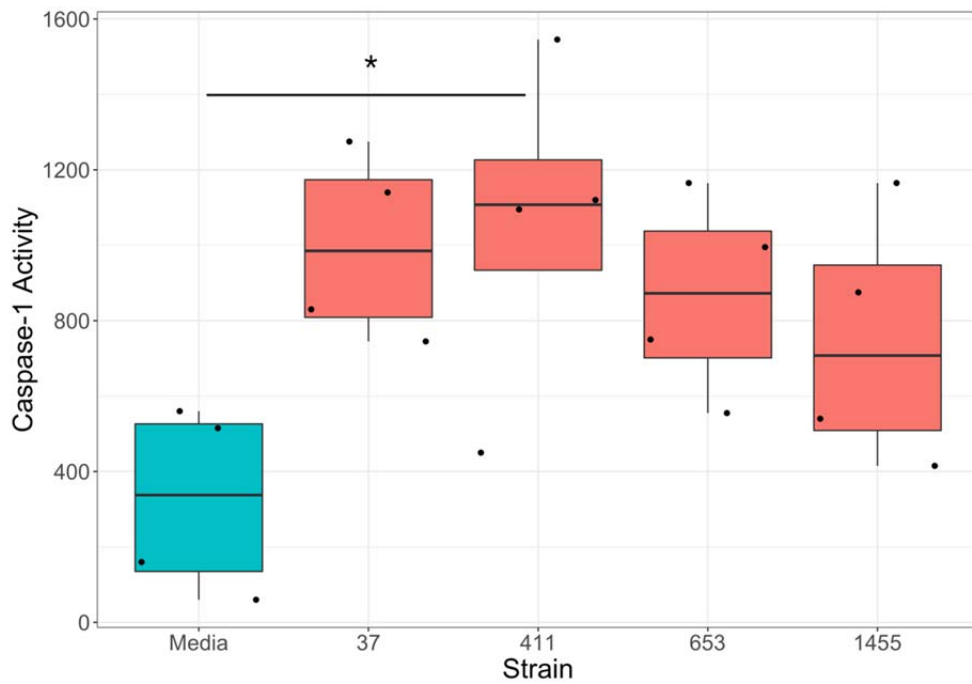
620

621

622

623

624



625

626 **Supplemental Figure 6: Bacteria induce caspase-1 activation in THP-1s**

627 THP-1 derived macrophages were unstimulated or treated with bacteria for 25 hours.

628 Supernatants were then assessed for caspase-1 activity using a caspase-1 GLO assay. Data

629 represent the amount of caspase-1 activity (caspase-1 activity = (RLU GLO) - (RLU AC)) from

630 paired samples. Individual black dots indicate a single biological replicate (n = 4 for each group).

631 Statistical significance is defined as p < 0.05 as calculated by ANOVA with a Tukey post-hoc and

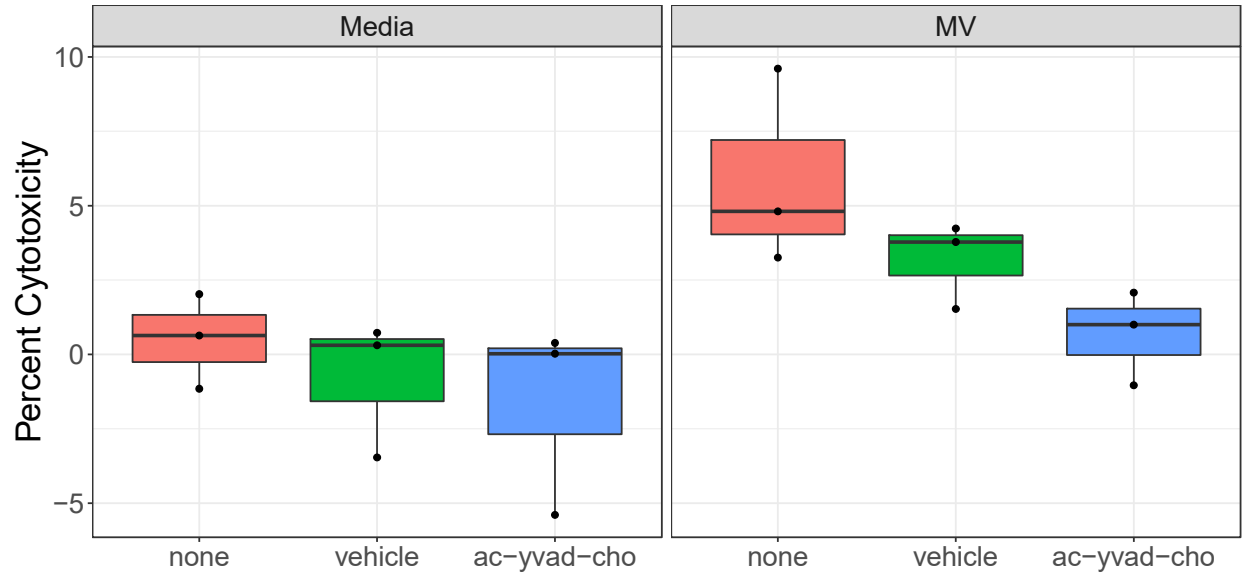
632 indicated by (\*).

633

634

635

636

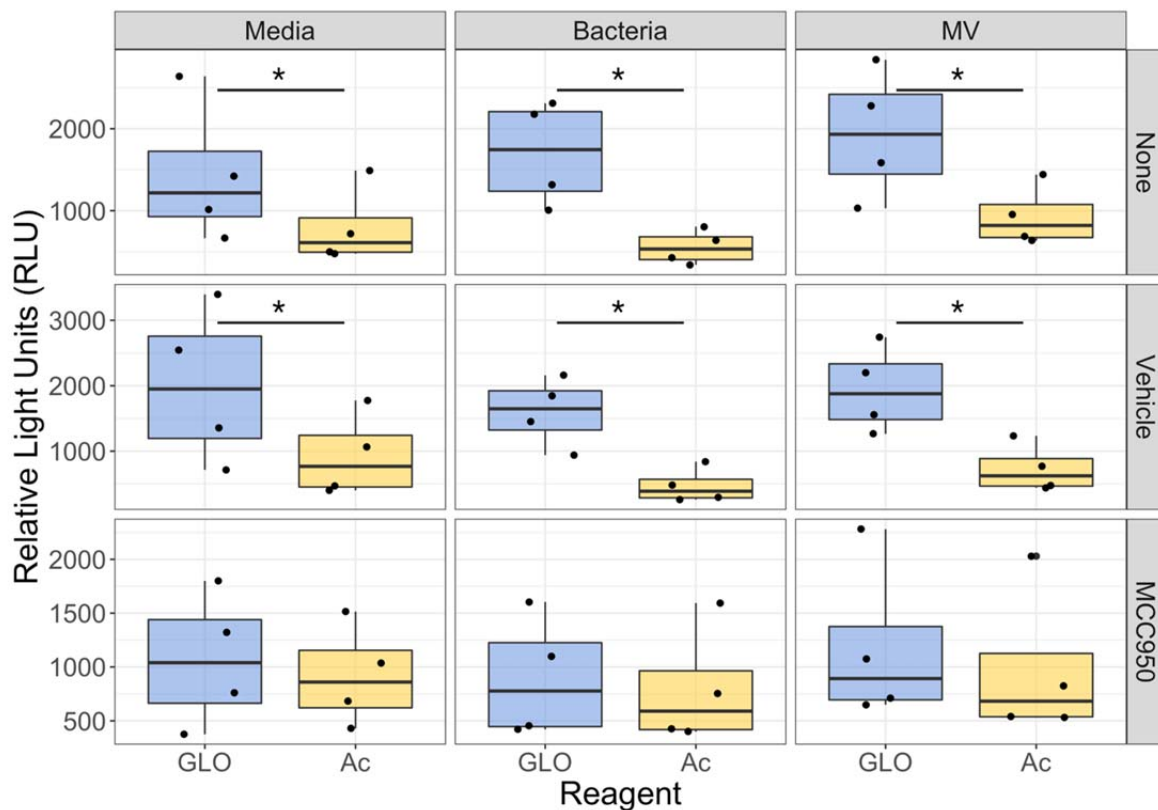


637  
638 **Supplemental Figure 7: Caspase-1 inhibition does not impact cell death responses**

639 THP-1s were untreated, treated with ethanol, or Ac-YVAD-CHO for 30 minutes. Supernatants  
640 from THP-1 derived macrophages, which were subsequently unstimulated or treated with MVs  
641 for 25 hours were assessed for cytotoxicity using the CyQuant LDH Assay. Individual black dots  
642 indicate a single biological replicate (n = 3 for each group). Statistics were determined using  
643 either an ANOVA with a Tukey HSD post hoc. No significant difference relative to non-  
644 pretreated cells were detected for either group.

645  
646  
647  
648  
649  
650  
651  
652  
653  
654  
655  
656  
657  
658  
659  
660

661  
662



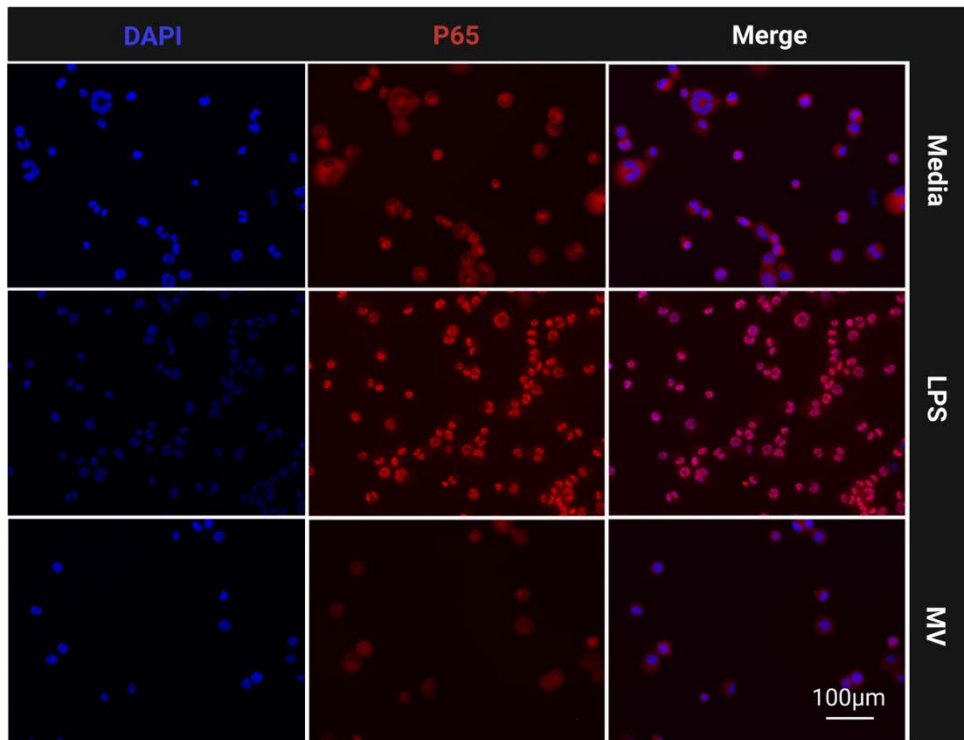
663  
664

665 **Supplemental Figure 8: Inhibition of NLRP3 prevents Caspase-1 Activation in Response to**  
666 **MVs**

667 THP-1s were treated with the NLRP3 inhibitor MCC950 prior to treatment with bacteria, MVs,  
668 or media. Caspase-1 activity was determined using the Caspase-1 GLO assay. Individual points  
669 represent individual biological replicates (n = 4 each group). Statistics were determined using an  
670 ANOVA with a Tukey's HSD post-hoc test. Significance was defined as  $p > 0.05$  and denoted  
671 with an (\*).

672  
673  
674  
675

676  
677  
678  
679  
680  
681  
682  
683  
684  
685  
686  
687  
688  
689  
690  
691  
692  
693  
694  
695  
696  
697  
698  
699  
700  
701  
702  
703  
704  
705  
706  
707  
708  
709  
710  
711  
712  
713  
714  
715  
716



### Supplemental Figure 9: MVs do not prime human macrophages

Differentiated THP-1 derived macrophages were untreated or treated with LPS or MVs for 30 minutes prior to fixation and immunofluorescence staining for NF- $\kappa$ B subunit p65 (stained red). Nuclei are stained using DAPI (blue). Shown here are representative images (n = 5) taken at 40x magnification.

717 **REFERENCES**

- 718
- 719 1. Verani JR, McGee L, Schrag SJ, Division of Bacterial Diseases NCFIARD, Centers for  
720 Disease Control and Prevention (CDC). 2010. Prevention of perinatal group B  
721 streptococcal disease--revised guidelines from CDC, 2010. *MMWR Recomm Rep* 59:1-  
722 36.
- 723 2. Doran KS, Nizet V. 2004. Molecular pathogenesis of neonatal group B streptococcal  
724 infection: no longer in its infancy. *Mol Microbiol* 54:23-31.
- 725 3. Bae GE, Yoon N, Choi M, Hwang S, Hwang H, Kim JS. 2016. Acute Placental Villitis as  
726 Evidence of Fetal Sepsis: An Autopsy Case Report. *Pediatr Dev Pathol* 19:165-8.
- 727 4. Anderson BL, Simhan HN, Simons KM, Wiesenfeld HC. 2007. Untreated asymptomatic  
728 group B streptococcal bacteriuria early in pregnancy and chorioamnionitis at delivery.  
729 *Am J Obstet Gynecol* 196:524.e1-5.
- 730 5. Jones N, Bohnsack JF, Takahashi S, Oliver KA, Chan MS, Kunst F, Glaser P, Rusniok C,  
731 Crook DW, Harding RM, Bisharat N, Spratt BG. 2003. Multilocus sequence typing  
732 system for group B streptococcus. *J Clin Microbiol* 41:2530-6.
- 733 6. Lin FY, Whiting A, Adderson E, Takahashi S, Dunn DM, Weiss R, Azimi PH, Philips  
734 JB, Weisman LE, Regan J, Clark P, Rhoads GG, Frasci CE, Troendle J, Moyer P,  
735 Bohnsack JF. 2006. Phylogenetic lineages of invasive and colonizing strains of serotype  
736 III group B Streptococci from neonates: a multicenter prospective study. *J Clin Microbiol*  
737 44:1257-61.
- 738 7. Luan SL, Granlund M, Sellin M, Lagergård T, Spratt BG, Norgren M. 2005. Multilocus  
739 sequence typing of Swedish invasive group B streptococcus isolates indicates a  
740 neonatally associated genetic lineage and capsule switching. *J Clin Microbiol* 43:3727-  
741 33.
- 742 8. Poyart C, Réglie-Poupet H, Tazi A, Billoët A, Dmytruk N, Bidet P, Bingen E, Raymond  
743 J, Trieu-Cuot P. 2008. Invasive group B streptococcal infections in infants, France.  
744 *Emerg Infect Dis* 14:1647-9.
- 745 9. Manning SD, Springman AC, Lehotzky E, Lewis MA, Whittam TS, Davies HD. 2009.  
746 Multilocus sequence types associated with neonatal group B streptococcal sepsis and  
747 meningitis in Canada. *J Clin Microbiol* 47:1143-8.
- 748 10. Flores AR, Galloway-Peña J, Sahasrabhojane P, Saldaña M, Yao H, Su X, Ajami NJ,  
749 Holder ME, Petrosino JF, Thompson E, Margarit Y Ros I, Rosini R, Grandi G,  
750 Horstmann N, Teatero S, McGeer A, Fittipaldi N, Rappuoli R, Baker CJ, Shelburne SA.  
751 2015. Sequence type 1 group B Streptococcus, an emerging cause of invasive disease in  
752 adults, evolves by small genetic changes. *Proc Natl Acad Sci U S A* 112:6431-6.
- 753 11. Manning SD, Lewis MA, Springman AC, Lehotzky E, Whittam TS, Davies HD. 2008.  
754 Genotypic diversity and serotype distribution of group B streptococcus isolated from  
755 women before and after delivery. *Clin Infect Dis* 46:1829-37.
- 756 12. Korir ML, Laut C, Rogers LM, Plemmons JA, Aronoff DM, Manning SD. 2017.  
757 Differing mechanisms of surviving phagosomal stress among group B Streptococcus  
758 strains of varying genotypes. *Virulence* 8:924-937.
- 759 13. Flaherty RA, Borges EC, Sutton JA, Aronoff DM, Gaddy JA, Petroff MG, Manning SD.  
760 2019. Genetically distinct Group B Streptococcus strains induce varying macrophage  
761 cytokine responses. *PLoS One* 14:e0222910.

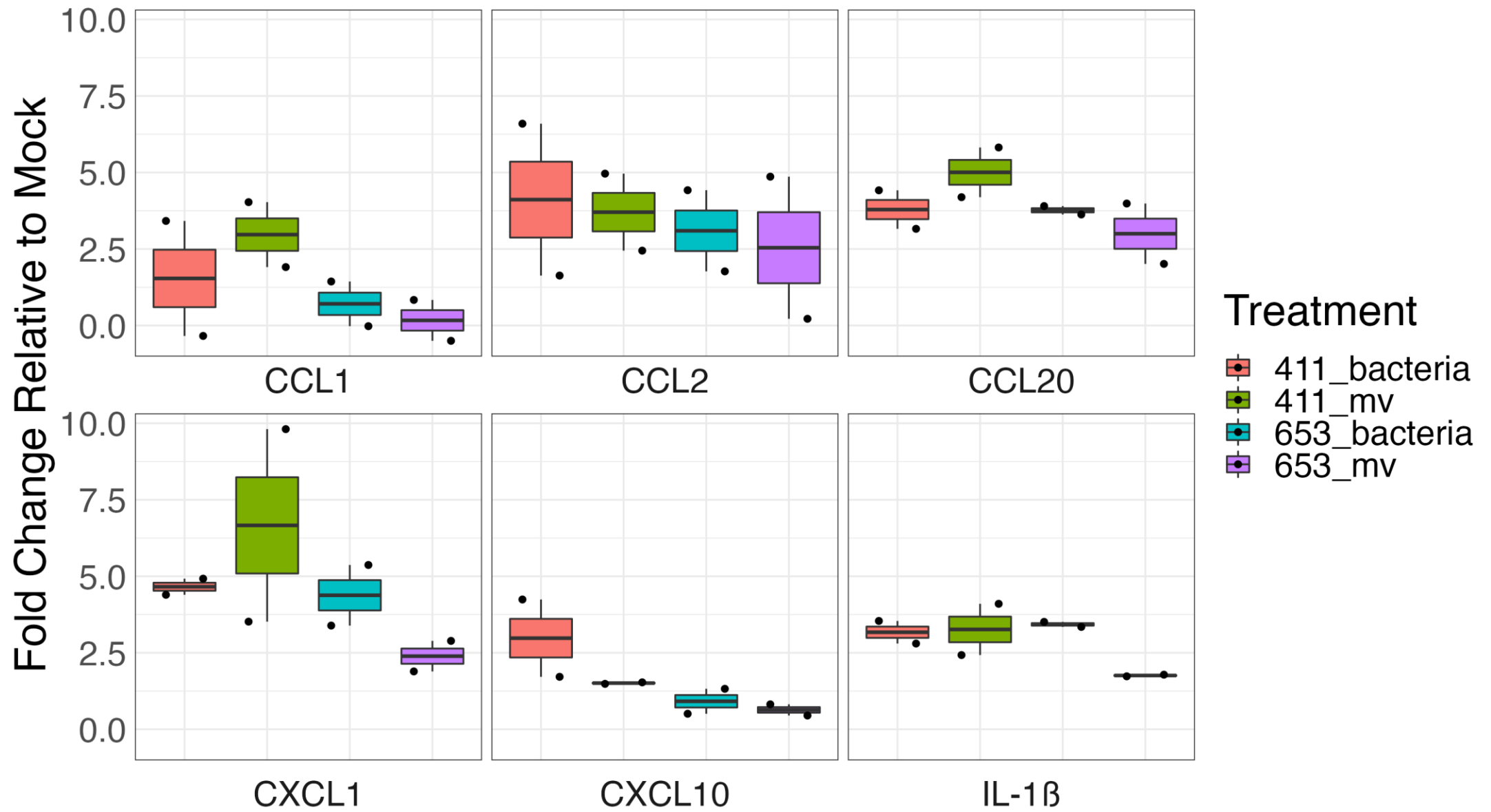
- 762 14. Springman AC, Lacher DW, Waymire EA, Wengert SL, Singh P, Zadoks RN, Davies  
763 HD, Manning SD. 2014. Pilus distribution among lineages of group b streptococcus: an  
764 evolutionary and clinical perspective. *BMC Microbiol* 14:159.
- 765 15. Springman AC, Lacher DW, Wu G, Milton N, Whittam TS, Davies HD, Manning SD.  
766 2009. Selection, recombination, and virulence gene diversity among group B  
767 streptococcal genotypes. *J Bacteriol* 191:5419-27.
- 768 16. Brochet M, Couvé E, Zouine M, Vallaëys T, Rusniok C, Lamy MC, Buchrieser C, Trieu-  
769 Cuot P, Kunst F, Poyart C, Glaser P. 2006. Genomic diversity and evolution within the  
770 species *Streptococcus agalactiae*. *Microbes Infect* 8:1227-43.
- 771 17. Surve MV, Anil A, Kamath KG, Bhutda S, Sthanam LK, Pradhan A, Srivastava R, Basu  
772 B, Dutta S, Sen S, Modi D, Banerjee A. 2016. Membrane Vesicles of Group B  
773 *Streptococcus* Disrupt Feto-Maternal Barrier Leading to Preterm Birth. *PLoS Pathog*  
774 12:e1005816.
- 775 18. De Paepe ME, Friedman RM, Gundogan F, Pinar H, Oyer CE. 2004. The histologic  
776 fetoplacental inflammatory response in fatal perinatal group B-streptococcus infection. *J*  
777 *Perinatol* 24:441-5.
- 778 19. Armistead B, Quach P, Snyder JM, Santana-Ufret V, Furuta A, Brokaw A, Rajagopal L.  
779 2021. Hemolytic Membrane Vesicles of Group B *Streptococcus* Promote Infection. *J*  
780 *Infect Dis* 223:1488-1496.
- 781 20. Biondo C, Mancuso G, Midiri A, Signorino G, Domina M, Lanza Cariccio V,  
782 Mohammadi N, Venza M, Venza I, Teti G, Beninati C. 2014. The interleukin-  
783 1 $\beta$ /CXCL1/2/neutrophil axis mediates host protection against group B streptococcal  
784 infection. *Infect Immun* 82:4508-17.
- 785 21. Lemire P, Roy D, Fittipaldi N, Okura M, Takamatsu D, Bergman E, Segura M. 2014.  
786 Implication of TLR- but not of NOD2-signaling pathways in dendritic cell activation by  
787 group B *Streptococcus* serotypes III and V. *PLoS One* 9:e113940.
- 788 22. McCutcheon CR, Pell ME, Gaddy JA, Aronoff DM, Petroff MG, Manning SD. 2021.  
789 Production and Composition of Group B Streptococcal Membrane Vesicles Vary Across  
790 Diverse Lineages. *Front Microbiol* 12:770499.
- 791 23. Houser BL. 2012. Decidual macrophages and their roles at the maternal-fetal interface.  
792 *Yale J Biol Med* 85:105-18.
- 793 24. Care AS, Diener KR, Jasper MJ, Brown HM, Ingman WV, Robertson SA. 2013.  
794 Macrophages regulate corpus luteum development during embryo implantation in mice. *J*  
795 *Clin Invest* 123:3472-87.
- 796 25. Rozner AE, Durning M, Kropp J, Wiepz GJ, Golos TG. 2016. Macrophages modulate the  
797 growth and differentiation of rhesus monkey embryonic trophoblasts. *Am J Reprod*  
798 *Immunol* 76:364-375.
- 799 26. Doster RS, Sutton JA, Rogers LM, Aronoff DM, Gaddy JA. 2018. *Streptococcus*  
800 *agalactiae* Induces Placental Macrophages To Release Extracellular Traps Loaded with  
801 Tissue Remodeling Enzymes via an Oxidative Burst-Dependent Mechanism. *mBio* 9.
- 802 27. Thomas JR, Appios A, Zhao X, Dutkiewicz R, Donde M, Lee CYC, Naidu P, Lee C,  
803 Cerveira J, Liu B, Ginhoux F, Burton G, Hamilton RS, Moffett A, Sharkey A, McGovern  
804 N. 2021. Phenotypic and functional characterization of first-trimester human placental  
805 macrophages, Hofbauer cells. *J Exp Med* 218.
- 806 28. Sutton JA, Rogers LM, Dixon BREA, Kirk L, Doster R, Algood HM, Gaddy JA, Flaherty  
807 R, Manning SD, Aronoff DM. 2019. Protein kinase D mediates inflammatory responses

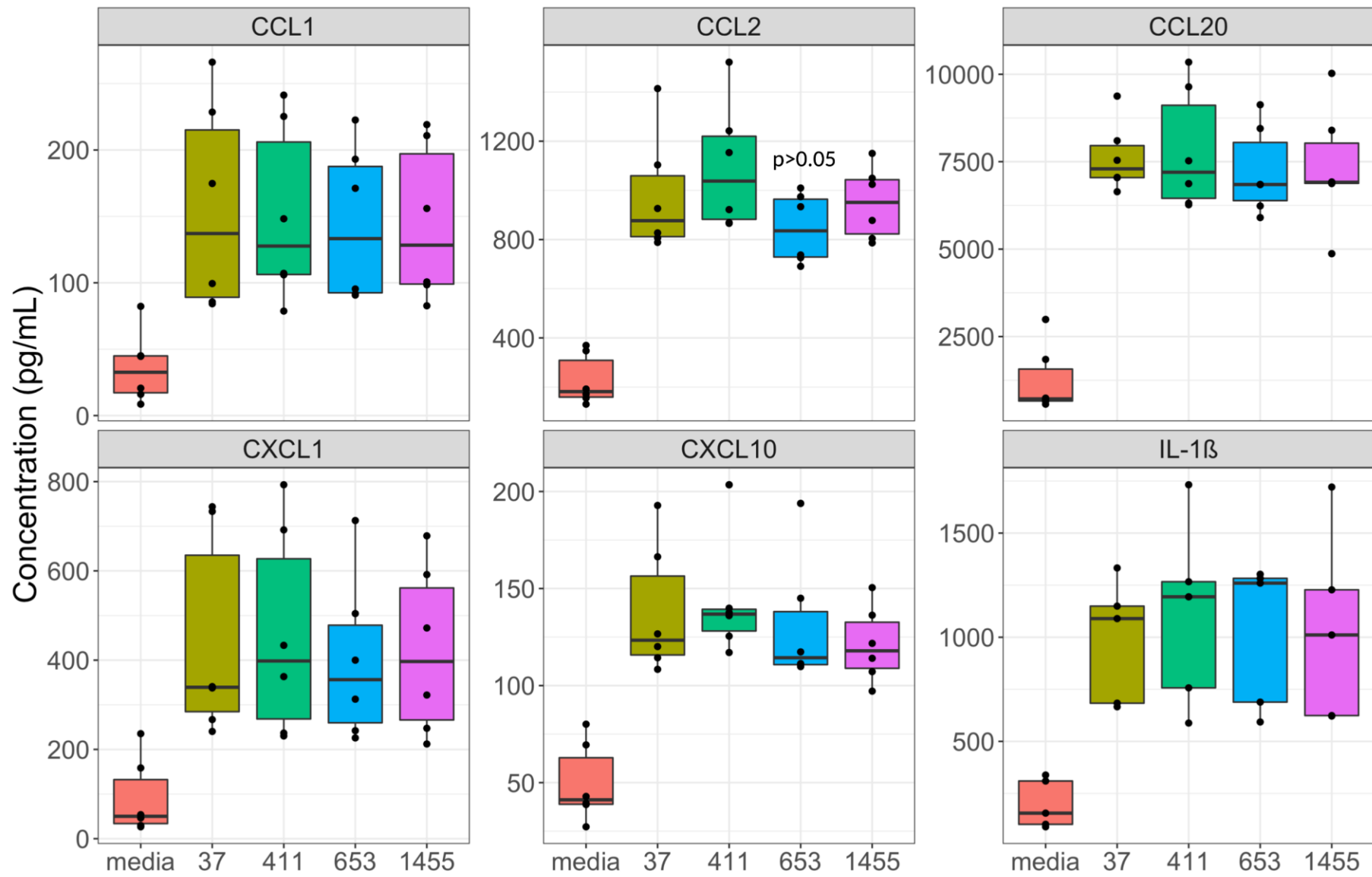
- 808 of human placental macrophages to Group B Streptococcus. *Am J Reprod Immunol*  
809 81:e13075.
- 810 29. Tsuchiya S, Kobayashi Y, Goto Y, Okumura H, Nakae S, Konno T, Tada K. 1982.  
811 Induction of maturation in cultured human monocytic leukemia cells by a phorbol diester.  
812 *Cancer Res* 42:1530-6.
- 813 30. Eastman AJ, Vrana EN, Grimaldo MT, Jones AD, Rogers LM, Alcendor DJ, Aronoff  
814 DM. 2021. Cytotrophoblasts suppress macrophage-mediated inflammation through a  
815 contact-dependent mechanism. *Am J Reprod Immunol* 85:e13352.
- 816 31. Davies HD, Adair C, McGeer A, Ma D, Robertson S, Mucenski M, Kowalsky L, Tyrell  
817 G, Baker CJ. 2001. Antibodies to capsular polysaccharides of group B Streptococcus in  
818 pregnant Canadian women: relationship to colonization status and infection in the  
819 neonate. *J Infect Dis* 184:285-91.
- 820 32. Spaetgens R, DeBella K, Ma D, Robertson S, Mucenski M, Davies HD. 2002. Perinatal  
821 antibiotic usage and changes in colonization and resistance rates of group B streptococcus  
822 and other pathogens. *Obstet Gynecol* 100:525-33.
- 823 33. Nguyen SL, Greenberg JW, Wang H, Collaer BW, Wang J, Petroff MG. 2019.  
824 Quantifying murine placental extracellular vesicles across gestation and in preterm birth  
825 data with tidyNano: A computational framework for analyzing and visualizing  
826 nanoparticle data in R. *PLoS One* 14:e0218270.
- 827 34. Nguyen SL, Ahn SH, Greenberg JW, Collaer BW, Agnew DW, Arora R, Petroff MG.  
828 2021. Integrins mediate placental extracellular vesicle trafficking to lung and liver in  
829 vivo. *Sci Rep* 11:4217.
- 830 35. Tsuchiya S, Yamabe M, Yamaguchi Y, Kobayashi Y, Konno T, Tada K. 1980.  
831 Establishment and characterization of a human acute monocytic leukemia cell line (THP-  
832 1). *Int J Cancer* 26:171-6.
- 833 36. Flaherty RA, Aronoff DM, Gaddy JA, Petroff MG, Manning SD. 2021. Distinct Group B.  
834 *Infect Immun* 89.
- 835 37. Costa A, Gupta R, Signorino G, Malara A, Cardile F, Biondo C, Midiri A, Galbo R,  
836 Trieu-Cuot P, Papasergi S, Teti G, Henneke P, Mancuso G, Golenbock DT, Beninati C.  
837 2012. Activation of the NLRP3 inflammasome by group B streptococci. *J Immunol*  
838 188:1953-60.
- 839 38. Jin L, Batra S, Douda DN, Palaniyar N, Jeyaseelan S. 2014. CXCL1 contributes to host  
840 defense in polymicrobial sepsis via modulating T cell and neutrophil functions. *J*  
841 *Immunol* 193:3549-58.
- 842 39. Ritzman AM, Hughes-Hanks JM, Blaho VA, Wax LE, Mitchell WJ, Brown CR. 2010.  
843 The chemokine receptor CXCR2 ligand KC (CXCL1) mediates neutrophil recruitment  
844 and is critical for development of experimental Lyme arthritis and carditis. *Infect Immun*  
845 78:4593-600.
- 846 40. Hieshima K, Imai T, Opdenakker G, Van Damme J, Kusuda J, Tei H, Sakaki Y,  
847 Takatsuki K, Miura R, Yoshie O, Nomiyama H. 1997. Molecular cloning of a novel  
848 human CC chemokine liver and activation-regulated chemokine (LARC) expressed in  
849 liver. Chemotactic activity for lymphocytes and gene localization on chromosome 2. *J*  
850 *Biol Chem* 272:5846-53.
- 851 41. Qian BZ, Li J, Zhang H, Kitamura T, Zhang J, Campion LR, Kaiser EA, Snyder LA,  
852 Pollard JW. 2011. CCL2 recruits inflammatory monocytes to facilitate breast-tumour  
853 metastasis. *Nature* 475:222-5.

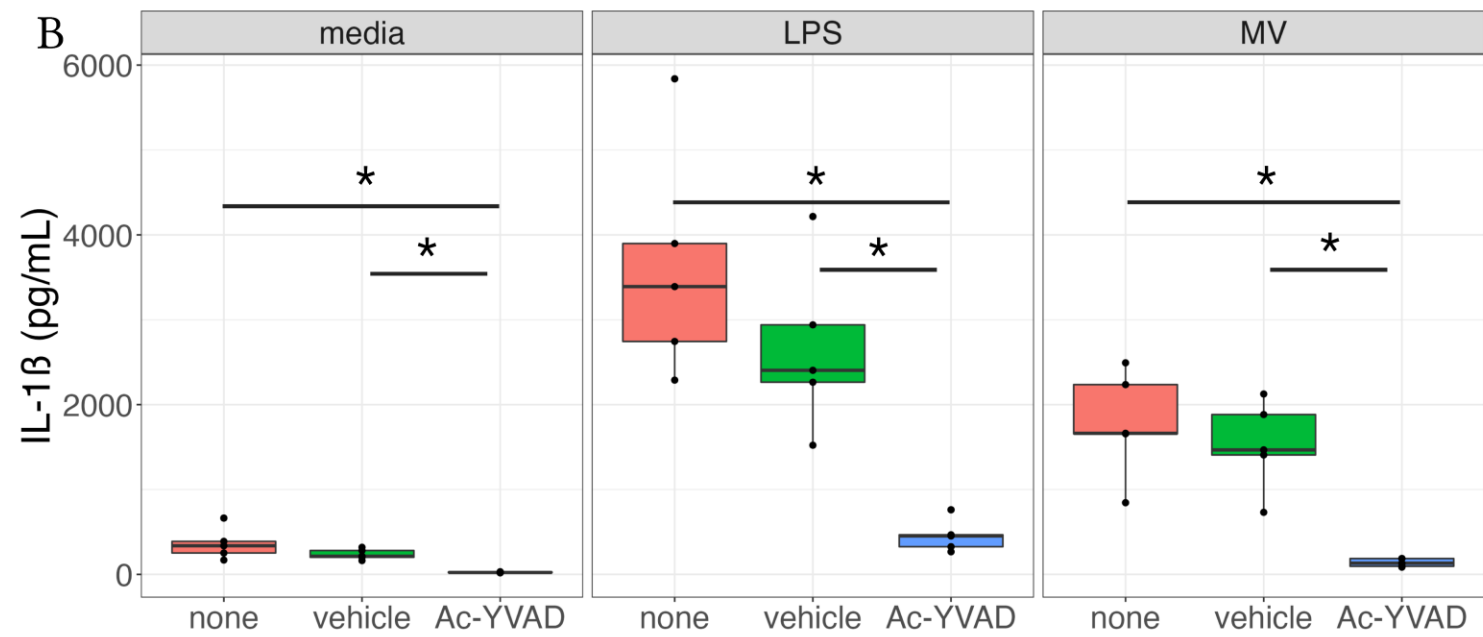
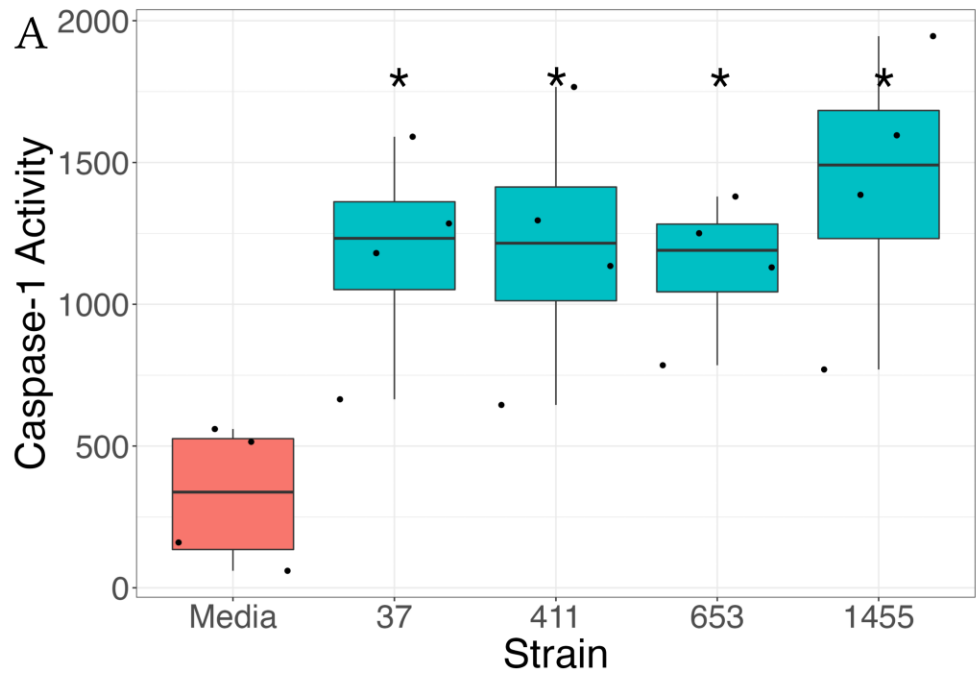


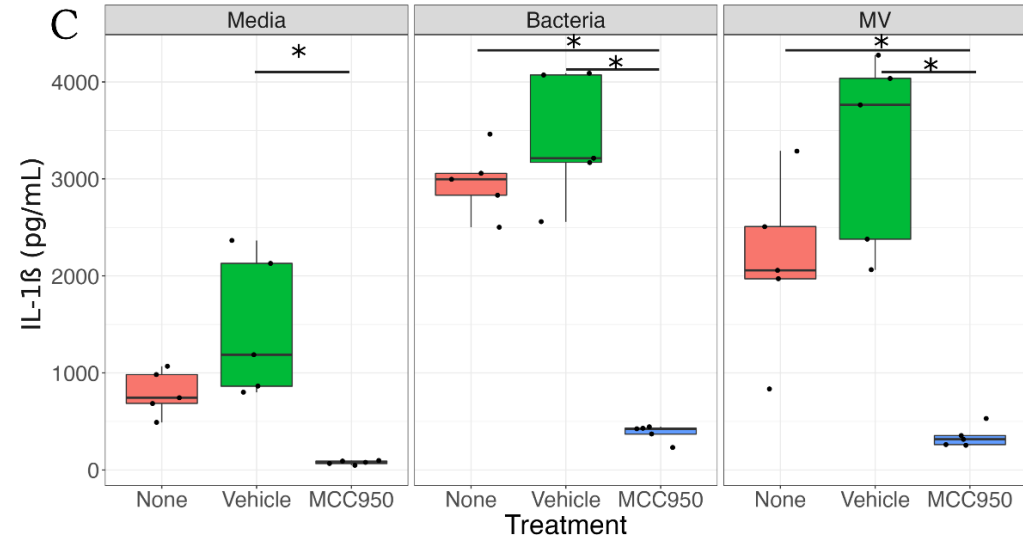
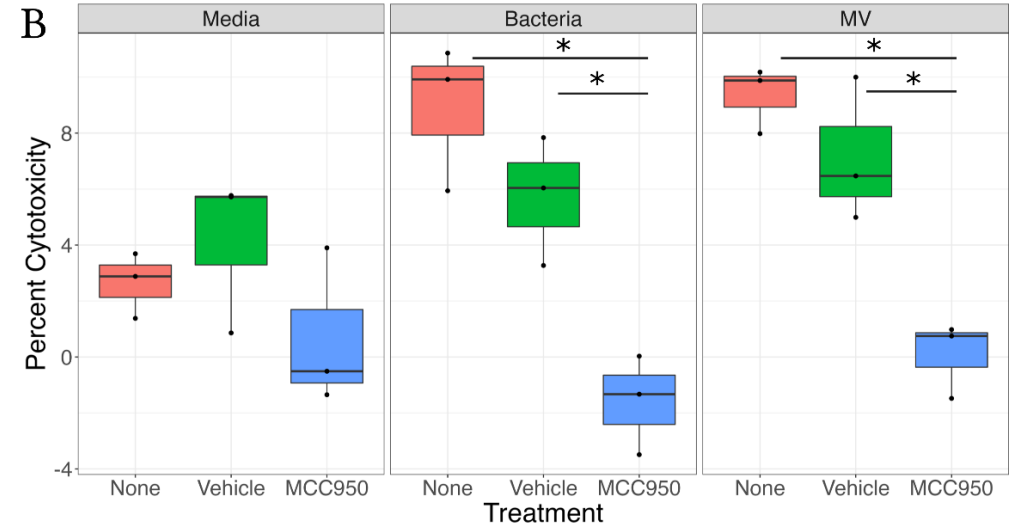
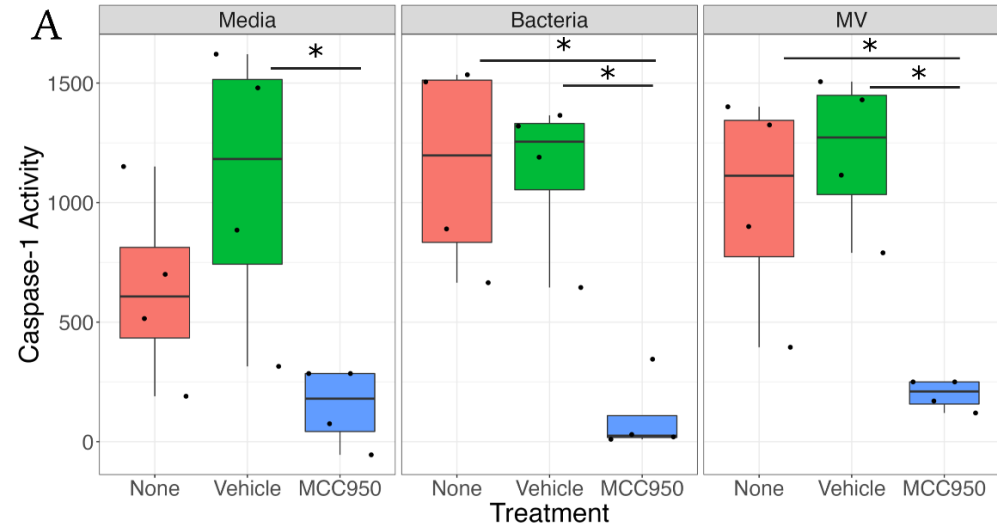
- 854 42. Cantor J, Haskins K. 2007. Recruitment and activation of macrophages by pathogenic  
855 CD4 T cells in type 1 diabetes: evidence for involvement of CCR8 and CCL1. *J Immunol*  
856 179:5760-7.
- 857 43. Liu M, Guo S, Hibbert JM, Jain V, Singh N, Wilson NO, Stiles JK. 2011. CXCL10/IP-10  
858 in infectious diseases pathogenesis and potential therapeutic implications. *Cytokine*  
859 *Growth Factor Rev* 22:121-30.
- 860 44. Kim BJ, Bee OB, McDonagh MA, Stebbins MJ, Palecek SP, Doran KS, Shusta EV.  
861 2017. Modeling Group B. *mSphere* 2.
- 862 45. Okazaki K, Kondo M, Kato M, Nishida A, Takahashi H, Noda M, Kimura H. 2008.  
863 Temporal alterations in concentrations of sera cytokines/chemokines in sepsis due to  
864 group B streptococcus infection in a neonate. *Jpn J Infect Dis* 61:382-5.
- 865 46. Biondo C, Mancuso G, Midiri A, Signorino G, Domina M, Lanza Cariccio V, Venza M,  
866 Venza I, Teti G, Beninati C. 2014. Essential role of interleukin-1 signaling in host  
867 defenses against group B streptococcus. *mBio* 5:e01428-14.
- 868 47. Berner R, Csorba J, Brandis M. 2001. Different cytokine expression in cord blood  
869 mononuclear cells after stimulation with neonatal sepsis or colonizing strains of  
870 *Streptococcus agalactiae*. *Pediatr Res* 49:691-7.
- 871 48. Kelley N, Jeltema D, Duan Y, He Y. 2019. The NLRP3 Inflammasome: An Overview of  
872 Mechanisms of Activation and Regulation. *Int J Mol Sci* 20.
- 873 49. Akira S, Takeda K. 2004. Toll-like receptor signalling. *Nat Rev Immunol* 4:499-511.
- 874 50. Takeuchi O, Akira S. 2002. MyD88 as a bottle neck in Toll/IL-1 signaling. *Curr Top*  
875 *Microbiol Immunol* 270:155-67.
- 876 51. Baeuerle PA, Baltimore D. 1988. Activation of DNA-binding activity in an apparently  
877 cytoplasmic precursor of the NF-kappa B transcription factor. *Cell* 53:211-7.
- 878 52. Zheng D, Liwinski T, Elinav E. 2020. Inflammasome activation and regulation: toward a  
879 better understanding of complex mechanisms. *Cell Discov* 6:36.
- 880 53. Yu HB, Finlay BB. 2008. The caspase-1 inflammasome: a pilot of innate immune  
881 responses. *Cell Host Microbe* 4:198-208.
- 882 54. Mariathasan S, Weiss DS, Newton K, McBride J, O'Rourke K, Roose-Girma M, Lee WP,  
883 Weinrauch Y, Monack DM, Dixit VM. 2006. Cryopyrin activates the inflammasome in  
884 response to toxins and ATP. *Nature* 440:228-32.
- 885 55. Sharma D, Kanneganti TD. 2016. The cell biology of inflammasomes: Mechanisms of  
886 inflammasome activation and regulation. *J Cell Biol* 213:617-29.
- 887 56. Broz P, Dixit VM. 2016. Inflammasomes: mechanism of assembly, regulation and  
888 signalling. *Nat Rev Immunol* 16:407-20.
- 889 57. Kostura MJ, Tocci MJ, Limjuco G, Chin J, Cameron P, Hillman AG, Chartrain NA,  
890 Schmidt JA. 1989. Identification of a monocyte specific pre-interleukin 1 beta convertase  
891 activity. *Proc Natl Acad Sci U S A* 86:5227-31.
- 892 58. Mohammadi N, Midiri A, Mancuso G, Patanè F, Venza M, Venza I, Passantino A, Galbo  
893 R, Teti G, Beninati C, Biondo C. 2016. Neutrophils Directly Recognize Group B  
894 *Streptococci* and Contribute to Interleukin-1 $\beta$  Production during Infection. *PLoS One*  
895 11:e0160249.
- 896 59. Whidbey C, Vornhagen J, Gendrin C, Boldenow E, Samson JM, Doering K, Ngo L,  
897 Ezekwe EA, Gundlach JH, Elovitz MA, Liggitt D, Duncan JA, Adams Waldorf KM,  
898 Rajagopal L. 2015. A streptococcal lipid toxin induces membrane permeabilization and  
899 pyroptosis leading to fetal injury. *EMBO Mol Med* 7:488-505.

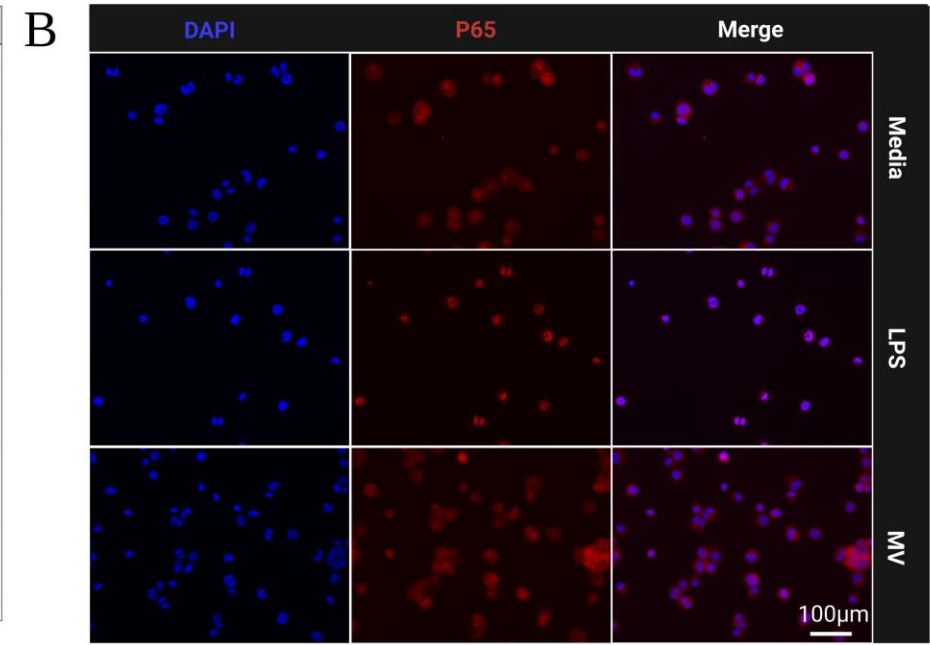
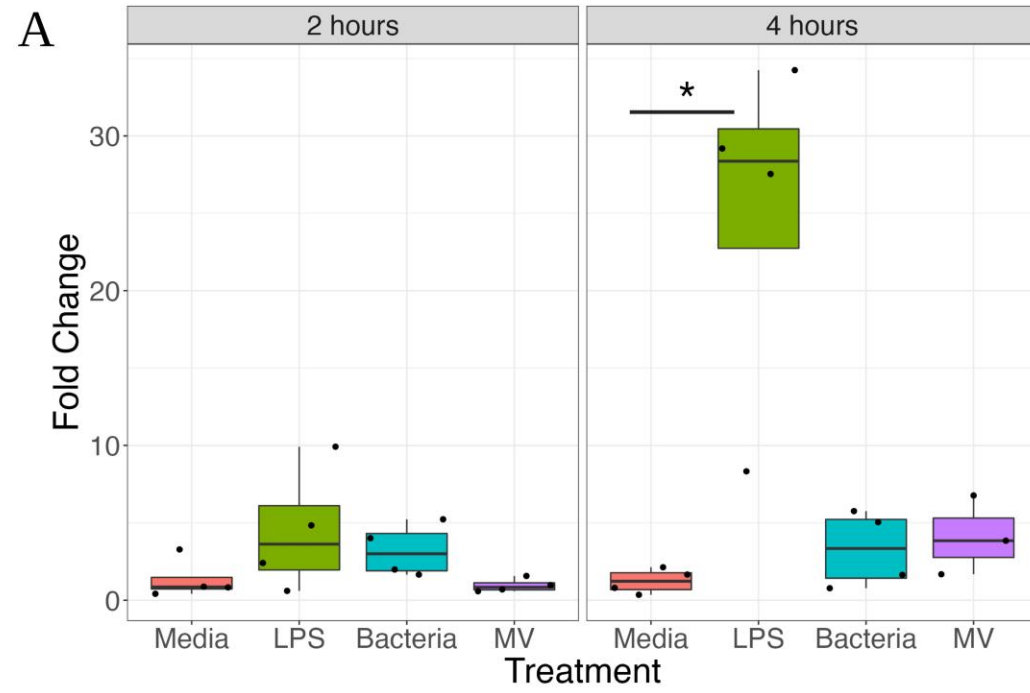
- 900 60. Gupta R, Ghosh S, Monks B, DeOliveira RB, Tzeng TC, Kalantari P, Nandy A,  
901 Bhattacharjee B, Chan J, Ferreira F, Rathinam V, Sharma S, Lien E, Silverman N,  
902 Fitzgerald K, Firon A, Trieu-Cuot P, Henneke P, Golenbock DT. 2014. RNA and  $\beta$ -  
903 hemolysin of group B Streptococcus induce interleukin-1 $\beta$  (IL-1 $\beta$ ) by activating NLRP3  
904 inflammasomes in mouse macrophages. *J Biol Chem* 289:13701-5.
- 905 61. Dubois H, Sorgeloos F, Sarvestani ST, Martens L, Saeys Y, Mackenzie JM, Lamkanfi M,  
906 van Loo G, Goodfellow I, Wullaert A. 2019. Nlrp3 inflammasome activation and  
907 Gasdermin D-driven pyroptosis are immunopathogenic upon gastrointestinal norovirus  
908 infection. *PLoS Pathog* 15:e1007709.
- 909 62. Swanson KV, Deng M, Ting JP. 2019. The NLRP3 inflammasome: molecular activation  
910 and regulation to therapeutics. *Nat Rev Immunol* 19:477-489.
- 911 63. Gendrin C, Vornhagen J, Armistead B, Singh P, Whidbey C, Merillat S, Knupp D, Parker  
912 R, Rogers LM, Quach P, Iyer LM, Aravind L, Manning SD, Aronoff DM, Rajagopal L.  
913 2018. A Nonhemolytic Group B Streptococcus Strain Exhibits Hypervirulence. *J Infect*  
914 *Dis* 217:983-987.
- 915 64. Chanput W, Mes JJ, Wichers HJ. 2014. THP-1 cell line: an in vitro cell model for  
916 immune modulation approach. *Int Immunopharmacol* 23:37-45.
- 917 65. Sawant KV, Poluri KM, Dutta AK, Sepuru KM, Troshkina A, Garofalo RP, Rajarathnam  
918 K. 2016. Chemokine CXCL1 mediated neutrophil recruitment: Role of  
919 glycosaminoglycan interactions. *Sci Rep* 6:33123.
- 920 66. Kothary V, Doster RS, Rogers LM, Kirk LA, Boyd KL, Romano-Keeler J, Haley KP,  
921 Manning SD, Aronoff DM, Gaddy JA. 2017. Group B. *Front Cell Infect Microbiol* 7:19.  
922



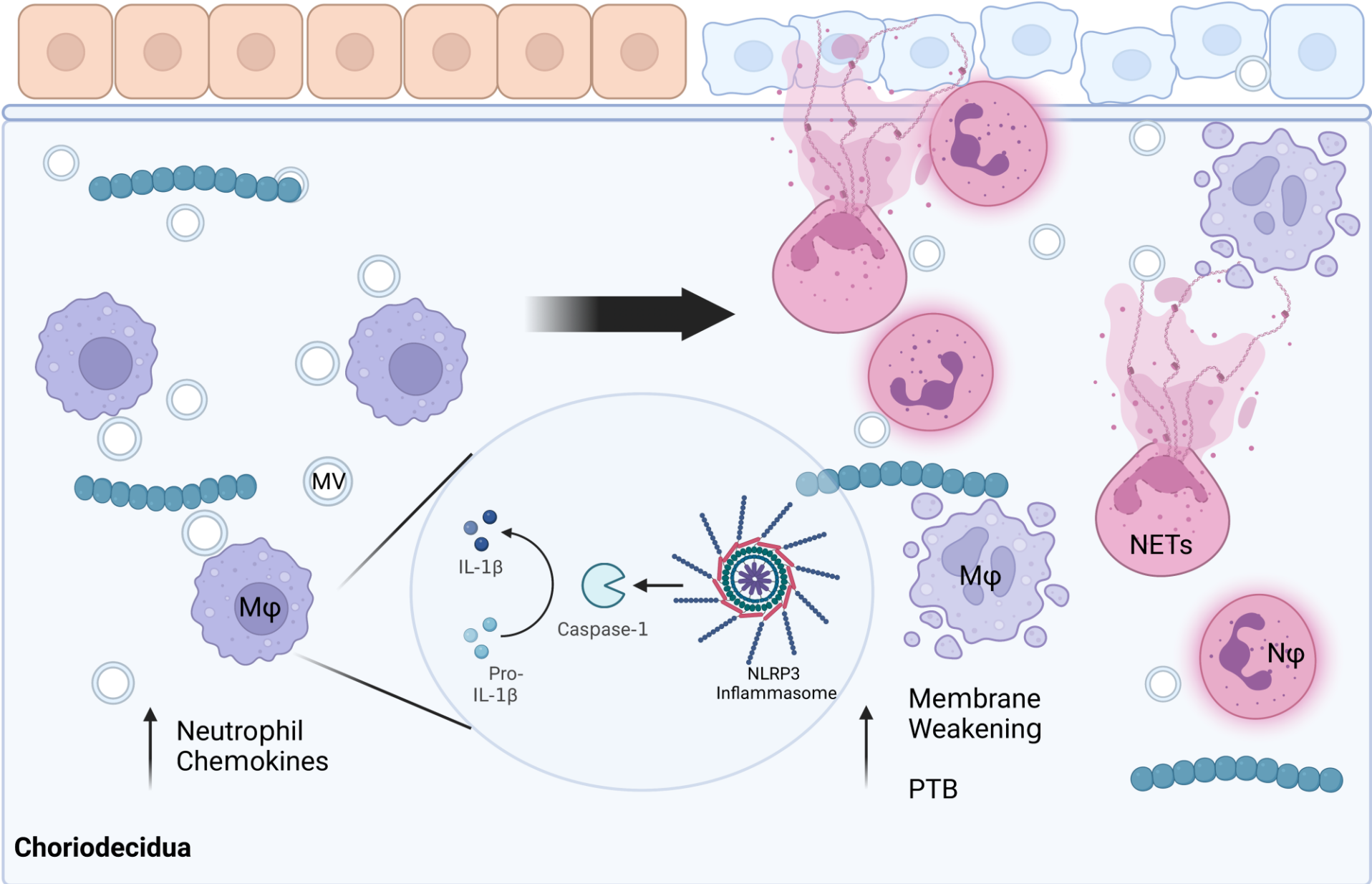








Amnion



Choriodecidia